WELCOME!

83rd Annual

PEC

PHYSICAL ELECTRONICS CONFERENCE

UW-La Crosse

July 31–August 3, 2023
University of Wisconsin-La Crosse

The 83rd Physical Electronics Conference, including the prestigious Nottingham Prize Competition for the best presentation based on doctoral research, will be held at the University of Wisconsin-La Crosse, July 31–August 3, 2023. This topical conference provides a yearly forum for the dissemination and discussion of novel and fundamental theoretical and experimental research in the physics, chemistry, biology, and engineering of surfaces and interfaces.

Abstract Booklet

Tuesday, August 1

9:00 am – 10:20 AM

Hall of Nations Room 1300

Centennial Hall

308 16th Street North | La Crosse, WI 54601

Oral Presentations

Session 1

Chair: Prof. Seth King, *University of Wisconsin – La Crosse*

Epitaxial Growth of Semiconducting Graphene Nanoribbons on Germanium Surfaces

R. M. Jacobberger

Department of Electrical and Computer Engineering, University of Wisconsin-Madison, 1415 Engineering Drive, Madison, WI, 53706, United States

Email: jacobberger@wisc.edu

Arrays of aligned semiconducting graphene nanoribbons with sub-5-nm widths and well-defined edges promise to meet the demands of speed, energy efficiency, density, and functionality required for next-generation semiconductor electronics. However, development of nanoribbon technologies has been inhibited by challenges in the industry-compatible production of nanoribbon arrays with high structural precision. Here, we present a bottom-up route to grow nanoribbons with tunable sub-5-nm widths, nearly atomically defined armchair edges, atomic thickness, unidirectional alignment, and controlled placement directly on conventional Ge or Ge/Si wafers via chemical vapor deposition (CVD) (Fig. 1) [1,2,3,4]. The precise control over the nanoribbon structure transforms graphene from a zero-bandgap semimetal into a semiconductor with a technologically useful bandgap > 0.5 eV. The nanoribbons exhibit high performance in field-effect transistors in terms of their on-state conductance (~10^3 μS μm^{-1}) and on/off current ratio (~10^4).

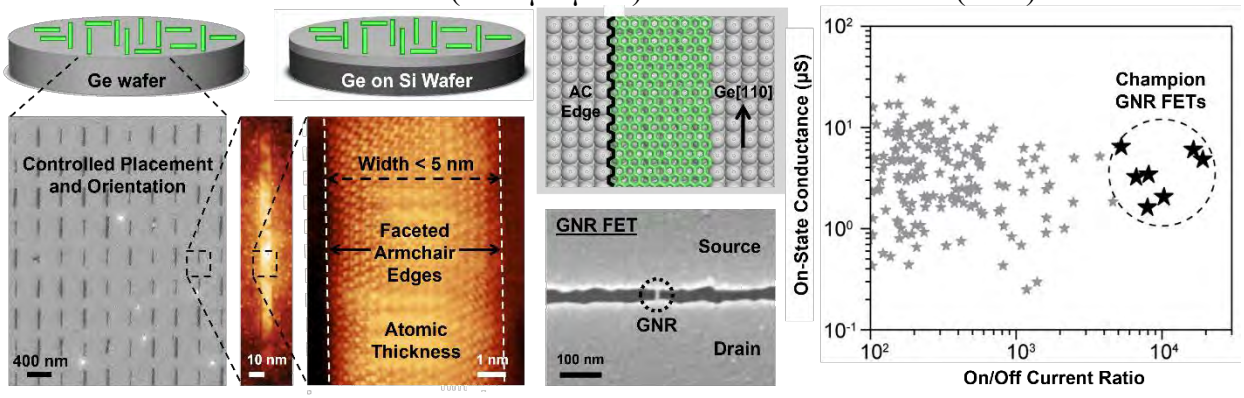

Fig. 1. Graphene nanoribbons (GNRs) grown on Ge and Ge/Si wafers via CVD have tunable sub-5-nm widths, atomically sharp armchair (AC) edges, and controlled placement and alignment in large-area arrays. The nanoribbons also exhibit promising performance in field-effect transistors (FETs) that rival state-of-the-art Si-based devices in on-state conductance and on/off current ratio.

References:

[1] R. M. Jacobberger, et al. *Nat. Commun.* **6**, 8006 (2015).
[2] R. M. Jacobberger, et al. *ACS Nano* **11**, 8924-8929 (2017).
[3] R. M. Jacobberger, et al. *Nanoscale* **11**, 4864-4875 (2019).
[4] A. J. Way, et al. *Nat. Commun.* **13**, 2992 (2022).

Preference: Oral

Atomic-scale manipulation of buried graphene – SiC interface by local electric field

M. Kolmer[1], J. Hall[1,2], S. Chen[1], Y. Han[1], M.C.Tringides[1,2]

[1]Ames National Laboratory, [2] Department of Physics, Iowa State University, Ames IA 50011
Email: mkolmer@ameslab.gov

Unprecedent precision of scanning tunneling microscopy (STM) enables control of matter at scales of single atoms. Nevertheless, fabrication of truly functional systems with STM encounters fundamental problems in the transition from atomic-scale manipulation strategies to practical devices. One of the primary concerns lies in protection of the designer structures formed atop the surface. In this context, STM manipulation of subsurface defects on technologically relevant materials is encouraging. However, due to the intrinsic, surface-sensitive nature of STM, such approaches require combination of refinements in design and synthesis to fully benefit from the precision of a scanning probe setup. Here, we propose a material platform and experimental protocols for ultimately precise manipulation of a buried interface [1]. We show that an electric field from the STM-tip reversibly controls local coupling between the graphene buffer layer and the SiC substrate under epitaxial bilayer graphene (BLG). This process is vertically defined by the atomically sharp interface, located ~1 nm below the top graphene layer, and laterally by single sites from its (6×6)SiC moiré lattice. We postulate that this highly reversible and local ferroelectric switching is based on the charge redistribution associated with breaking and restoring the corresponding C-Si covalent bonds. The switching is enhanced by the intrinsic, tensile interface strain. The results present a novel architecture for local patterning of epitaxial graphene heterostructures, or other two-dimensional materials in general, from structural engineering of the buried interfaces.

Pre-print publication

[1] M. Kolmer, J. Hall, S. Chen, Y. Han, M.C. Tringides "Atomic-scale manipulation of buried graphene – SiC interface by local electric field", 21 July 2023, PREPRINT available at Research Square [https://doi.org/10.21203/rs.3.rs-3136595/v1]

Band structure tuning of 2-d intercalated quantum materials and nanographenes

M. Kolmer[1], S. Chen[1], Y. Han[1], Y. Luan[1,2], J. Hall[1,2], Z. Fei[1,2], L.L. Wang[1], J. W. Evans[1,2], M.C.Tringides[1,2]

[1]Ames National Laboratory, [2] Department of Physics, Iowa State University, Ames IA 50011
Email: mkolmer@ameslab.gov

The goals of our activities are the tunable synthesis and characterization of nanoscale structures with predictive control of their morphology and geometry, to realize novel types of 2-d quantum materials. We focus on several graphene-based materials to establish the underlying principles for controlling their dimensions, structural uniformity, interface quality and interatomic interactions. Materials include: (i) on-demand metal-graphene heterostructures grown by targeted metal intercalation, with precise experimental tuning of metal location [1-5] (ii) Nanographene (NG) and graphene nanoribbons (NGR) generated by on-surface synthesis utilizing programmable chemical reactions of organic precursors, an ideal playground to test quantum materials physics in atomically precise systems. We realize targeted electronic band structures by developing synthesis protocols to control the bonding of the deposited atoms at pre-designed locations based on in-situ surface diffraction (LEED) and scanning tunneling microscopy (STM). Post growth characterization of the targeted band structures with spectroscopic techniques (scanning tunneling spectroscopy (STS), photoemission spectroscopy (ARPES), scanning near-field optical microscopy (SNOM)) is used to confirm targeted electronic effects. Density functional theory modelling is applied both to optimize synthesis, to attain predictiveness in the growth and to validate the expected band structure modifications.

Recent Publications

[1] Y. Luan, M. Kolmer, M.C. Tringides, Z. Fei, "Nanoscale infrared imaging and spectroscopy of hot-electron plasmons in graphene", *Phys. Rev. B* **107**, 085414 (2023).

[2] Y. Han, M. Kolmer, M.C. Tringides, JW Evans "Thermodynamics and kinetics of Pb intercalation under graphene on SiC (0001)" *Carbon* **5** 336 (2023).

[3] S. Chen, Y. Han, M. Kolmer, J. Hall, M. Hupalo, J.W. Evans, M.C. Tringides "Targeted Dy intercalation under graphene/SiC for tuning its electronic band structure" *Phys. Rev. B* **107**, 045408 (2023)

[4] M. Kolmer, B. Schrunk, M. Hupalo, J. Hall, S. Chen, J. Zhang, C.-Z. Wang, A. Kaminski, M.C. Tringides, "Highly Asymmetric Graphene Layer Doping and Band Structure Manipulation in Rare Earth–Graphene Heterostructure by Targeted Bonding of the Intercalated Gadolinium", *J. Phys. Chem. C*. **126**, 6863 (2022).

[5] M. Kolmer, W. Ko, J. Hall, S. Chen, J. Zhang, H. Zhao, L. Ke, C.Z. Wang, A.P. Li, M.C. Tringides "Breaking of Inversion Symmetry and Interlayer Electronic Coupling in Bilayer Graphene Heterostructure by Structural Implementation of High Electric Displacement Fields" *J. Phys. Chem. Lett*. **13**, 11571-11580 (2022).

[6] M. Kolmer *et al.* "Rational synthesis of atomically precise graphene nanoribbons directly on metal oxide surfaces" *Science* **369,** 571-575 (2020)

[7] M. Kolmer *et al.*, "Fluorine-programmed nanozipping to tailored nanographenes on rutile TiO_2 surfaces" *Science* **363**, 57-60 (2019)

Electronic Transport and Polarization-Dependent Photoresponse in HfS_3 Nanoribbons

A. Lipatov,[1] J. Abourahma,[2] G. Viswan,[3] K. Acharya,[4] T. R. Paudel,[4] M. J. Loes,[2]

S. Bagheri,[2] P. A. Dowben,[3] and A. Sinitskii[2]

[1] Department of Chemistry, Biology and Health Sciences, South Dakota School of Mines and Technology, Rapid City, SD 57701, USA

[2] Department of Chemistry, University of Nebraska-Lincoln, Lincoln, NE 68588, USA

[3] Department of Physics and Astronomy, University of Nebraska-Lincoln, Lincoln, NE 68588, USA

[4] Department of Physics, South Dakota School of Mines and Technology, Rapid City, SD 57701, USA

Email: Alexey.Lipatov@sdsmt.edu

The transition metal trichalcogenide (TMTC) family of materials, such as TiS_3, ZrS_3, and HfS_3, provides an attractive platform for a variety of optoelectronic applications due to the presence of quasi-one-dimensional (quasi-1D) covalently bonded chains that can be mechanically exfoliated and used as nanoribbon-like transistor channels. In this paper, we report on the electrical characterization of field-effect transistors based on exfoliated few-layer HfS_3 nanoribbons and show that they exhibit a highly polarization-dependent photoresponse. If measured in air, the devices show a p-type response, which is likely caused by physisorbed and chemisorbed oxygen species. In a vacuum, the devices exhibit an n-type conductivity and a large photoresponse to white light and several lasers with wavelengths in the visible range of the spectrum. We also provide computational insights into the properties of HfS_3 that are relevant to device fabrication and electrical measurements. Theoretical calculations demonstrate that the exfoliation of HfS_3 flakes from bulk crystals is a facile process. We also show that direct and indirect band gaps are present in both monolayer and few-layer HfS_3 crystals and decrease with the number of layers. In addition to the experimental polarization-dependent photoresponse measurements of HfS_3 devices, we also attempted to gain insights into the photoexcitation process by a spectroscopic study of the unoccupied states of HfS_3.

Preference: oral

Single-crystalline Ru nanowires: Engineering & investigating interconnects beyond diffusive transport constraints

W.E. Kaden,[1] Q. Cumston,[2] A. Hegazy,[1] M. Daughtry,[1] E. Yi,[3] K. Barmak,[3] and K.R. Coffey[4]

[1]Department of Physics, University of Central Florida, 4111 Libra Drive, Orlando, FL 32816, USA

[2]Department of Electrical and Computer Engineering, University of Central Florida, 4328 Scorpius Street, Orlando, FL 32816, USA

[3]Department of Applied Physics and Applied Mathematics, Columbia University, 500 West 120th Street, New York, NY 10027, USA

[4]Department of Materials Science and Engineering, University of Central Florida, 12760 Pegasus Drive, Orlando, FL 32816, USA

Email: william.kaden@ucf.edu

Increasing resistivity of polycrystalline copper interconnects as wire width and height drop to and below the electron mean free path (EMFP) with Moore's law scaling has long been known as the gating factor limiting microprocessor clock speed and, more recently, power consumption/heat generation. However, soon this scaling can lead to a paradigm shift as the ***lengths*** of the interconnects also approach and drop below EMFP dimensions. Shorter transport length presents an opportunity to leverage ballistic [1] contributions to conductance to achieve energy-efficient computing, but only to the extent that non-phonon contributions to nanowire resistivity (primarily electron scattering from surfaces and grain boundaries) can be minimized. This additional scattering decreases the effective EMFP, restricting the potential for ballistic and partial ballistic transport to occur. Scattering from grain boundaries, which single-crystal nanowires will not contain, has been attributed to more than half of the copper resistivity increases relevant to polycrystalline interconnects. While experimental evidence of ballistic transport has been studied and successfully modelled at point contacts (often formed by deliberately crashing an STM tip into a conducting support to form point contacts of ill-defined shape and cross-sectional area), device scale demonstrations of this phenomenon and complications arising from mixed mode transport within nanowires of well-defined dimensions have thus far gone unreported. In this presentation, we will present structure-conductivity relationships for Ru(0001) thin-films and nanowires of varied dimensions to explore and further develop existing models of transport in the near/sub-EMFP size regime. This will include a phenomenological study of changes in surface-scattering specularity as a function of changes in processing conditions, and evidence suggestive of the onset of low-temperature, ballistic transport through sub-100 nm long Ru nanowires grown and patterned on Al_2O_3(0001) substrates. Figure 1 exhibits preliminary transport data collected from defect-rich nanowires, where the increasing room temperature vs. liquid helium resistivity ratio is consistent with increased ballistic contributions to low-temperature transport as wire length decreases below the 4.2 K EMFP.

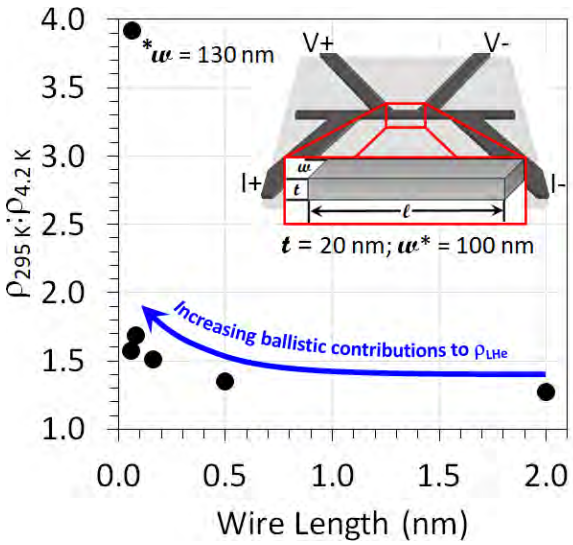

Fig. 1. Single-crystalline Ru/Al_2O_3(0001) nanowire device layout (inset) and length-dependent variation in measured resistivity ratio.

Preference: ORAL

[1] Ballistic conduction is non-ohmic and quantum limited by the wire area and number of electron channels. It is independent of wire length. A nanowire with fully ballistic transport will have a conductance two or three orders of magnitude higher than bulk ohmic conductance in the wire.

Tuesday, August 1

11:00 AM – 12:00 PM

Hall of Nations Room 1300

Centennial Hall

308 16th Street North | La Crosse, WI 54601

Oral Presentations

Session 2

Chair: Prof. Nan Jiang, *University of Illinois Chicago*

GaN Vacuum Nanoelectronics

George T. Wang[1], Keshab R. Sapkota[1], A. Alec Talin[2], Francois Leonard[2], Gyorgy Vizkelethy[1]

[1]Sandia National Laboratories, Albuquerque, NM 87185

[2]Sandia National Laboratories, Livermore, CA 94550

Email: gtwang@sandia.gov

*Invited Abstract

On-chip, field emission based vacuum nanoelectronic devices have the potential to combine advantages of traditional vacuum electron devices (e.g. vacuum tubes), such as robustness in harsh environments and high frequency operation, together with those of solid-state devices, such as size, integrability, and energy efficiency. By shrinking the vacuum channel to nanoscale dimensions well below the electron mean free path in air, these devices can operate at ambient pressures while maintaining the physical advantages of ballistic vacuum transport, thus potentially mitigating the need for vacuum packaging. We propose GaN as a superior materials platform compared to silicon or metals for solid-state, nanogap field emission devices based on its lower electron affinity, higher chemical stability, high breakdown voltage, and radiation hardness. Here, we demonstrate novel GaN nanogap field emission diodes that exhibit ultra-low turn-on voltage, high field emission current, and excellent on-off ratio. The devices are created using a two-step top-down approach allowing for the necessary sidewall verticality and surface smoothness. We present experimental and modeling results on the field emission characteristics of these devices at various nanogap sizes and operating pressures. The radiation hardness of these devices will also be discussed. These results provide critical new insights into the behavior of this new class of devices and point to future challenges and opportunities. *Sandia National Laboratories is managed and operated by NTESS under DOE NNSA contract DE-NA0003525.*

Electrical measurement methods with interdigitated electrode (IDE) arrays to identify metal-organic framework samples' protonic/electronic conduction mechanisms.

Özgür Yavuzçetin[1], Gündoğ Yücesan[2,3]

[1]Department of Physics, University of Wisconsin-Whitewater, Whitewater, WI 53190, United States

[2]Technische Universität Berlin, Lebensmittelchemie und Toxikologie, Berlin, Germany

[3]Heinrich-Heine-Universität Düsseldorf Institut für Anorganische Chemie und Structurechemie, Düsseldorf, Germany

E-mail: yavuzceo@uww.edu

Semiconducting layered materials are used in various essential applications, including light harvesting, optoelectronics, light emitting devices, transistors, supercapacitor electrodes, and sensing. Recently, metal-organic frameworks (MOFs) have been developed as novel microporous semiconductors with applications in supercapacitors and electrocatalysts for water splitting. MOFs offer a more comprehensive range of structural diversity than other layered material families due to the possibility of using many inorganic building units (IBUs) to construct novel MOF structures.

Standard electrical characterization techniques, such as the Van der Pauw method and two- or four-probe pellet methods, are commonly used to understand the conduction mechanisms of MOFs. However, these methods can introduce technical challenges, such as small contact areas and high resistance due to unmatched work functions.

In addition to supercapacitor and battery applications, MOFs can also be used in chemiresistive sensing fields, which require two-dimensional exposed areas with electrical contact from the electrodes. Gold interdigitated electrode (IDE) arrays are ideal test platforms for MOFs in chemiresistive sensing fields because they offer large exposed areas and good electrical contact.

In this work, we will present two electrical measurement methods, AC and DC, using IDE arrays to identify the protonic/electronic conduction mechanisms of IBUs. Our measurements indicate that the resistance of MOF samples is affected by hydration which involves both bulk and contact resistance and double-layer capacitance. The combined results of our DC and AC measurements suggest that the conduction in MOF samples involves electronic and ionic conduction.

References:

[1] Yucesan et. al., A new family of layered metal-organic semiconductors: Cu/V-organophosphonates, Small, 2023 (accepted for publication)

Preference: oral

Tuesday, August 1

1:20 PM – 2:40 PM

Hall of Nations Room 1300

Centennial Hall

308 16th Street North | La Crosse, WI 54601

Oral Presentations

Session 4

Chair: Prof. Robert Jacobberger, *University of Wisconsin – Madison*

Area-Selective Deposition/Patterning of Boron Carbide Layers: Etch Studies

Raja Sekhar Bale,[1] Rupak Thapa,[1] Anthony Caruso,[1] Sean King,[2] and Michelle Paquette[1]

[1]School of Science and Engineering, University of Missouri- Kansas City, 801 E 51st St, Kansas City, MO 64110, USA

[2]Logic Technology Development, Intel Corporation, 5200 NE Elam Young Parkway, Hillsboro OR 97124, USA

Email: rbr34@umsystem.edu

The semiconductor industry is pushing the boundaries of device scaling by way of novel processing methods and increasingly complex patterning schemes. This requires a variety of functional and patterning-assist materials as well as advanced deposition techniques. For years, silicon-based materials have been used to meet these needs; however, these alone cannot fulfill the range of material requirements moving forward. Boron carbide has shown promise due to its compelling dielectric, thermal, mechanical, chemical, and etch properties. Toward applying this material to next-generation integration schemes, we have been exploring the potential of going beyond traditional growth processes (e.g., plasma-enhanced chemical vapor deposition) and investigating innovative area-selective atomic layer deposition (AS-ALD) strategies. Herein we explore schemes for the selective dielectric on metal/dielectric deposition of boron carbide using monolayer and layer-by-layer methods. In particular, we focus on etch studies (wet and dry) toward understanding the stability and removal of these layers. X-ray photoemission spectroscopy (XPS), scanning electron microscopy (SEM), and atomic force microscopy (AFM) techniques are employed for the characterization and imaging of the resulting surfaces.

Preference: Oral

Abstract for PEC 2023

In-Plane and Out-of-Plane Magnetic Behavior in Iron Borate Single Crystal

Jacob Pfund[1], Jacob Franklin[1], Joshua Bedard[1], Ilya Sochnikov[1,2] and Menka Jain[1,2]

[1]*Department of Physics, University of Connecticut*, *Storrs, CT 06269*

[2]*Institute of Materials Science, University of Connecticut*, *Storrs, CT 06269*

Iron Borate ($FeBO_3$) is a unique material with promising applications in magnetic memory and magneto-optical devices. Single crystal of FeBO3 is transparent and green with rhombohedral calcite-type structure (space group D_{3d}^6). It is a room temperature ferromagnet with an optical band gap of 2.9 eV and plate-like growth. Neutron studies have shown that $FeBO_3$ becomes antiferromagnetic (AFM) below T_N ~348 K, with weak ferromagnetism in which the magnetic moments of the sublattice lie in the basal plane. However, there is lack of in-plane and out-of-plane magnetic data at low temperatures. In this work, we present the detailed in-plane and out-of-plane magnetic behavior in single crystal of $FeBO_3$. Temperature-dependent magnetic measurements show applied magnetic field dependent behavior at low temperatures (T< 25 K). Low temperature SQUID images are presented to identify the canting of magnetic moments and novel behavior near the ground state. Detailed magnetic properties, such as magnetic moment, exchange interaction parameters, and canting angles are also calculated.

Investigating Cr Based MBene and MXene using *first-principles* methods

Paromita Dutta[1], Turan Birol[1] and Deniz Çakur[2]

[1]Department of Chemical Engineering and Materials Science, University of Minnesota, Minneapolis, MN 55455, USA
[2] Department of Physics and Astrophysics, University of North Dakota, Grand Forks, North Dakota 58202, USA

Email: pdutta@umn.edu

MXenes and MBenes are an emerging class of 2D ternary transition metal compounds (carbides, nitrides, borides) that share layered structures. This class of materials are synthesized from selective chemical etching of a series of $M_{n+1}AX_n$ phases (called MAX and MAB phases) where M is an early transition metal, A is element from groups (12-16) and X is C/N/B. These 2D structures have a chemical formula of $M_{n+1}X_nT_2$ where T is surface terminating group (F, Cl, Br and I). They hold promise and attracted recent attention owing to their various applications in spintronics, quantum computing, optoelectronics and energy storage. MAX and MAB have shown different electronic properties which led to their intensive studies despite having similar crystal structures. MBenes also have similar crystal structures as MXenes yet their theoretical studies are relatively fewer than MXenes. Recently, MAX and MAB phases have shown significant electronic correlations. This implies there is a possibility of witnessing the changes in the electronic correlations when one changes the slab thickness and the surface terminations. In this context, we will be presenting a comparative study of Cr based MBene and MXene using Density functional theory and Dynamical mean field theory.

Preference: Oral

First-principles investigation of mechanical, thermal, oxidation and doping properties of MoAlB

Bipasa Samanta,[1] Salawu Omotayo Akande,[1] Cem Sevik, [2] and Deniz Çakir[1]

[1]Department of Physics and Astrophysics, University of North Dakota, Grand Forks, ND, 58202, United States of America

[2]Department of Physics & NANOlab Center of Excellence, University of Antwerp, Eskisehir Technical University, 26555 Eskisehir, Turkey

Email: bipasa.samanta@und.edu

Ternary nano-laminated transition metal borides, referred to as MAB phases, are a group of compounds that exhibit remarkable thermal, mechanical, and electronic properties. To develop useful practical applications of them, understanding their properties at fundamental level is crucial. With this motivation we have carried out a detailed understanding of the mechanical, thermal and oxidation properties of most renowned member of the MAB phase family: MoAlB. Through our first principle calculations, we have studied electron-phonon coupling, thermal conductivity, thermal expansion, and mechanical properties and established a relationship between strain and phonon behavior through quasi-harmonic approximation. The results obtained show the dependence of the properties on the strain axis and hence the anisotropic nature of MoAlB. Apart from being mechanically strong, MoAlB is also known for its excellent resistance to oxidation, attributed to the formation of a protective Al_2O_3 layer on its surface. Through surface energy, defect energy and Gibbs free energy calculation, we show that indeed Al_2O_3 is prominent intermediate, either direct or through various steps. Further, molecular dynamics simulations confirmed that the oxidation of MoAlB surfaces is a complex process that depends highly on the surface termination. Apart from studying the properties of MoAlB, we have also ventured in finding new $Mo_{1-x}M'_xAlB$ phases (M'=transition metal) with better mechanical and thermal properties and stability. Doping is one of the most applied techniques and using cluster expansion method, we generated structures with different concentrations of M' atoms. To evaluate the formation enthalpy of $Mo_{1-x}M'_xAlB$ alloys, we investigated the impact of various entropy contributions, including configurational, electronic, and vibrational entropy. Of all we found that configurational entropy plays a significant role in stabilizing the random phases. We also observe that while W is soluble across the entire range of mixing ratios, Sc and Ti are completely insoluble in any ratio. On the other hand, Cr, Ta, Nb, and V can be successfully incorporated into the MoAlB lattice in varying fractions at elevated temperature. Our study provides valuable insight into the stability, structural properties, and oxidation behavior of MoAlB surfaces and $Mo_{1-x}M'_xAlB$ phases at the atomic level. Our motive is to guide the design and engineering of these materials to tailor their properties for specific applications based on the need of the applicator.

References:

[1] S. Kota, M. Agne, E. Zapata-Solvas, O. Dezellus, D. Lopez, B. Gardiola, M. Radovic, and M. W. Barsoum, Physical Review. B. 95, 144108 (2017).

[2] J. Mou, S. Li, B. Yao, P. Ma, W. Yu, Y. Zhou, I. Smokovych, and M. Scheffler, Journal of Alloys and Compounds, 831, 154802 (2020).

Poster Abstracts

SURFACE CHEMISTRY OF ZIRCONIUM BOROHYDRIDE ON ZIRCONIUM DIBORIDE (0001).

Ayoyele Ologun

University of Illinois Chicago

Zirconium diboride ZrB_2 is an extremely hard material with a high melting point of 3246 °C; given these properties, ZrB_2 can be used for various applications, such as high-resistant coatings for body armors and tanks. In addition, it has also been explored as a diffusion barrier in microelectronics. Industrially, highly conformal thin films of ZrB_2 are grown via chemical vapor deposition (CVD), using zirconium borohydride $Zr(BH_4)_4$ as a precursor. While surface chemistry plays a central role in the CVD of ZrB_2 from the $Zr(BH_4)_4$ precursor, the surface mechanism is yet to be explored. In this study, we investigated the surface mechanism of $Zr(BH_4)_4$ decomposition on a ZrB_2(0001) surface with reflection absorption infrared spectroscopy (RAIRS), temperature-programmed desorption (TPD), and X-ray photoelectron spectroscopy (XPS). The RAIRS spectra obtained on exposing the ZrB_2(0001) surface at 90K to $Zr(BH_4)_4$(g) closely matched that of the pure compound, indicating adsorption of $Zr(BH_4)_4$ without decomposition. However, new surface intermediates were formed upon heating to 280 K, as shown by the retention of the vB-Ht stretch (2569 cm^{-1}) and δH-B-H bend (-1228 & 1057 cm^{-1}) in the RAIRS spectra. These surface intermediates were tentatively identified as either BH_4 or BH_3 and were found stable up to 330 K. Temperature-programmed desorption studies revealed the desorption of B_2H_6 and H_2 at around 470 K.

P2

Electrochemical Conversion of Carbon Dioxide to value-added chemicals on copper-based alloys

James Bartsch[1], Meredith Zannacker[1], Dong Hun Lee[2], Sunghwan Lee[2] and Sujat Sen[1]

[1]Department of Chemistry and Biochemistry, University of Wisconsin La Crosse, 54601
[2]School of Engineering Technology, Purdue University, West Lafayette, IN 47907

Email: jbartsch@uwlax.edu

Copper has been investigated extensively as an electrocatalyst for the conversion of Carbon dioxide (CO_2) to a variety of hydrocarbon products at room temperature. Alloys of copper (Cu) with metals such as silver (Ag) or tin (Sn) have also been shown to economically useful products such as ethylene, methane or formate with tunable selectivity between the same, depending on the composition of the alloy. Furthermore, varying the particle size, surface morphology, texture, and porosity of these catalysts have also been shown to dramatically change its electrocatalytic properties and product distribution.

In this work, we utilize thin layers of copper, silver and specific combinations of the same on both metal and gas-diffusion layer (GDL) substrates. Detailed characterization of these metal coated substrates has been done through scanning electron microscopy (SEM) as well as Energy-dispersive X-ray (EDX) analysis to determine relative ratios of the metals present. Herein, we present preliminary results showing the electrocatalytic performance of these metal films for the conversion of CO_2 inside both liquid-fed conventional H-Cell reactors using both cyclic voltammetry and chronoamperometry testing over 1-hour long electrolysis. Product analysis is performed through NMR for liquid phase products and GC-FID/TCD for gas-phase products. We also present on the characterization of these films after the electrolysis to understand changes to the metal surface and morphology.

Preference: poster

The Development of ZnO, Ultraviolet, All-Optical Switches

B. W. Gagner, J. R. Stevenson, S. T. King, and E. J. Gansen

Department of Physics, University of Wisconsin – La Crosse,
1725 State Street, La Crosse, WI, 54601, USA
Email: gagner9733@uwlax.edu

The pursuit of high-speed communication has driven the development of new optoelectronic components, such as all-optical, surface-normal, switches constructed of semiconductor thin-film heterostructures. In such a device, a strong control pulse and a weaker signal pulse are spatially overlapped in the heterostructure [Fig. 1(a)] and tuned to the band edge of the active semiconductor layer [Fig. 1(b)]. The control modulates the transmission of the signal by altering the absorption properties of the semiconductor. ZnO is a promising material for switches that operate in the ultraviolet (UV) region. It has a bandgap of ~3.4 eV and is less toxic than other materials with similar bandgaps, such as GaN. The structures we are studying are composed of alternating layers of polycrystalline ZnO and $Zn_{0.9}Mg_{0.1}O$, where the ZnO serves as the active semiconductor layer.

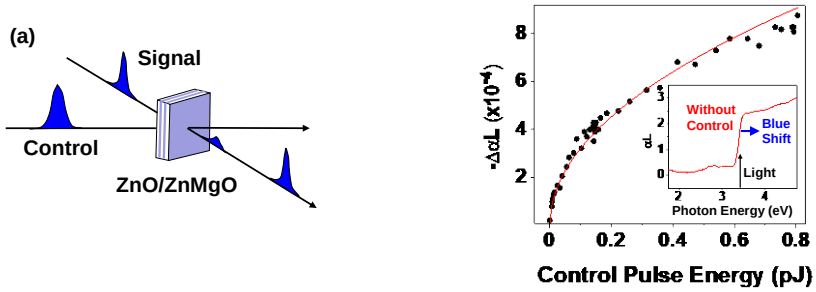

Figure 1. (*a*) All-optical surface-normal switch. (*b*) Control-induced change in absorbance ($\Delta\alpha L$) as a function of control pulse energy for coincident control and signal pulses. *Inset*: The absorbance (αL) of the $ZnO/Zn_{0.9}Mg_{0.1}O$ heterostructure as a function of photon energy in the absence of the control pulse.

Here, we investigate the absorption changes of $ZnO/Zn_{0.9}Mg_{0.1}O$ heterostructures with varying layer thicknesses using 120-ps light pulses. In these experiments, we measure the absorption changes as a function of the energy, polarization, repetition rate, and time delay of the control and signal pulses. Our experiments indicate that the switching action is produced when the conduction-band electrons and valence-band holes excited by the control separate due to a built-in electric field in the ZnO layers [1]. The resulting space-charge field screens the built-in field, blue shifting the band edge by reducing the excitonic red shift associated with the quantum-confined Stark effect [2]. In our presentation, we will discuss how the carrier dynamics impact the switch's speed.

References:

[1] T. Makino et al., Semicond. Sci. Technol. **20**, S78-S91 (2005).
[2] D. A. B. Miller et al., Phys. Rev. B **32**, 1043-1060 (1985).

Preference: poster

Growth of Pd Nanoclusters on Single-Layer Graphene on Ir (111)

Buddhika S. A. Gedara, Shilpa Choyal, Nan Jiang, and Michael Trenary

Department of Chemistry, University of Illinois at Chicago, 845 West Taylor Street, Chicago, Illinois 60607

Email: awijen2@uic.edu

Metal nanoclusters formed on graphene or graphene-oxide templates have garnered significant attention in recent years. They have been extensively studied due to their wide range of applications in catalysis, biosensing, semiconductor devices, hydrogen storage, and electron transport. Nucleation and growth of Pd nanoclusters on a single-layer of graphene on the Ir(111) surface have been studied using scanning tunneling microscopy (STM). Dendritic Pd islands are grown on the Ir(111) surface, while triangular-shaped Pd clusters are grown on the graphene surface. Due to weak interaction between the underlying graphene and the Pd, Pd clusters are removed by the STM tip as shown in Fig. 1. This allows us to find the nucleation site of the Pd clusters on the supercell of the moiré superstructure. The lattice mismatch between the graphene layer and the underlying substrate surface gives rise to moiré structures, providing a variety of binding sites for adatoms and small clusters. We found that the Pd clusters nucleate at fcc sites (where the center of the graphene ring is located above the fcc hollow site of Ir(111)) on graphene.

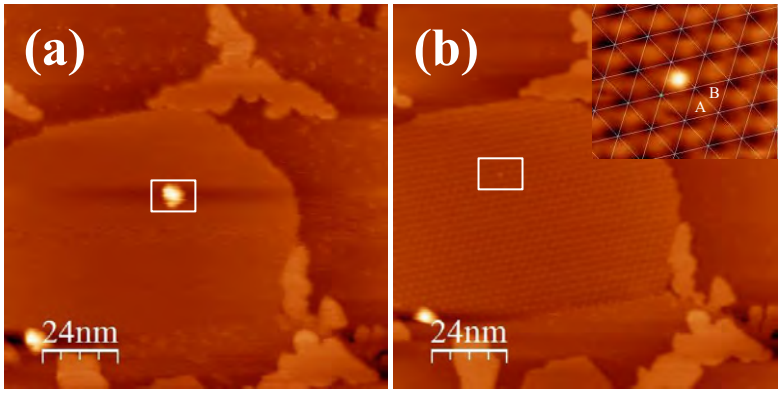

Figure 1. (a) A downward-pointing triangular Pd cluster on graphene is shown within the white rectangle box. (b) The Pd cluster has been removed from the graphene surface by the tip due to a weak interaction between the underlying graphene. The nucleation site of the Pd cluster is still visible as it presumably still contains few Pd atoms, and the inset demonstrates that this site is the fcc site (fcc and hcp regions are indicated by the A and B labels, respectively in the inset of (b)) on the supercell of the moiré superstructure. Images were recorded at 0.2 nA and 2.0 V in a 120×120 nm^2 area.

Preference: poster

Investigation of SiO_2 Thin Film Resistance and Capacitance Using X-ray Photoelectron Spectroscopy

M. Carlos[1], I. Thomas[1], O. Nuri[1]

[1]Department of Physics and Astrophysics, University of North Dakota, Grand Forks, ND 58202

Email: carlos.munoz@und.edu

Knowledge of the electronic properties of materials at interfaces is paramount to the development of novel devices and creating new technologies that leverage those properties. Additionally understanding how radiation can damage these devices has importance in space applications and other high radiation environments. Using an XPS (x-ray photoelectron spectroscopy) method we developed for thin film silicon nanoparticles (SiNPs) [1] we measured the electronic characteristics of Silicon dioxide (SiO_2) films grown on p-type and n-type Si(001) samples. By applying DC or AC external bias, we were able to extract the resistance and capacitance of the oxide layer using the shifts in the binding energy of Si 2p peak. The measurement consists of the application of 10V DC or AC square wave pulses of 10V amplitude to the sample at various frequencies ranging from 400μHz to 1kHz. Measurements were also repeated under different X-ray intensities to quantify the effect of radiation on the electronic properties of the sample.

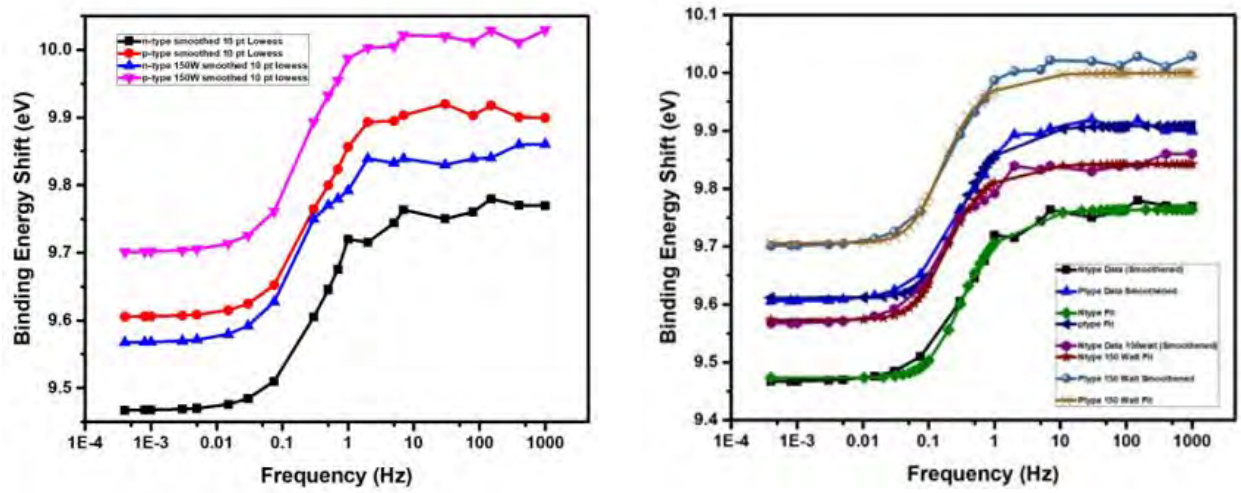

Fig. 1: Shift in binding energy vs. frequency

References:

[1] Laudari, A., Pathiranage, S., Thomas, S. A., Petersen, R. J., Anderson, K. J., Pringle, T. A., Hobbie, E. K., & Oncel, N. (2022). Probing electrical properties of a silicon nanocrystal thin film using x-ray photoelectron spectroscopy. *Review of Scientific Instruments*, *93*(8), 083906.

Preference: poster

Characterization of Polycrystalline Hf-doped Ga_2O_3

S.E. Chamberlain[1], V. Singh[1], and S.T. King[2]

[1]Department of Physics, Washington and Jefferson College, Washington, PA

[2]Department of Physics, University of Wisconsin – La Crosse, La Crosse, WI

Previous work has shown low concentrations of hafnium (Hf) incorporated into Ga_2O_3 single crystals act as a shallow donor, increasing carrier concentration and lowering the resistivity of the crystal [1,2]. However, only a single concentration of Hf was considered within these studies. To investigate the impact that Hf concentration has on the optical, structural, and morphological properties of the material, polycrystalline films of Hf-doped Ga_2O_3 were deposited at room temperature by reactive RF-sputtering onto silicon and fused silica substrates with varying concentrations of Hf, and were subsequently characterized by spectroscopic ellipsometry, UV-Vis spectrophotometry, x-ray diffraction, x-ray photoelectron spectroscopy, and atomic force microscopy.

Initial results show that all films, regardless of Hf concentration, are initially amorphous, but crystalize as β-Ga_2O_3 upon subsequent annealing, with the possibility of phase segregation when Hf concentrations reach approximately 3 at.%, giving an indication as to the solubility limit of Hf in Ga_2O_3. Spectroscopic ellipsometry measurements show that the index of refraction of the film is altered by Hf incorporation, while UV-Vis measurements show that the optical bandgap is not significantly altered. These results suggest that Hf-doped Ga_2O_3 may find use in optoelectronic devices and applications.

[1] https://iopscience.iop.org/article/10.1088/1361-6641/ab75a6

[2] https://aip.scitation.org/doi/10.1063/5.0062739

Substrate and annealing effects on PtNi films for high temperature electronics applications

M.Awais,[1] Morton Greenslit,[2] Matthew Cote,[2] Luke Doucette,[2] M.P da Cunha,[2] Robert J.Lad,[2] S.Hollen.[1]

Department of Physics and Astronomy, University of New Hampshire, DeMeritt Hall, 9 Library Way, Durham, NH 03824, USA.[1]

Department of Physics & Astronomy, University of Maine, Orono ME 04469-5708, USA.[2]

Email: muhammadawais.fiaz@unh.edu

Many technologies require thin film electrodes that can operate at high temperatures e.g., wireless microwave acoustic harsh environment temperature sensors, surface acoustic wave (SAW) devices and sensors [1]. These devices need electrodes which can withstand high temperatures without surface degradation and destroying their conductivity. Film morphology, especially upon annealing, is important to understand to optimize the performance of these electrodes. Thin films of Platinum Nickel (PtNi) alloy is a promising candidate for electrodes of these devices due to its high melting point and low resistance [2]. We investigated thin films of PtNi (Pt 90% Ni 10%) with thickness of 100 nm on Langasite and Sapphire substrates with 10 nm thick Zr adhesion layer in between substrate and films. PtNi films were deposited by the electron beam co-vapor deposition (PVD). We studied the effect of substrate and annealing on the morphology of PtNi films by using atomic force microscope (AFM) in contact mode and scanning tunneling microscope (STM) of sample with Sapphire substrate with annealing from 100 ºC to 800 ºC. We also did X-Ray photoelectron spectroscopic (XPS) analysis of thin films to confirm the percentage composition of thin films on both substrates. The results show that grain size and roughness of PtNi films on Sapphire substrate is bigger than on Langasite substrate as shown by the AFM images in Fig-1. In our annealing experiment we heated the film on Langasite substrate in UHV at a pressure 8×10^{-10} Torr and at the temperature of 100ºC for 5 minutes. AFM image of Langasite in fig-1 reveals that the grain size increased due to annealing effect. This agglomeration of PtNi particles due to heating has motivated us to study the samples at further higher temperatures. We will go up to 800 ºC in our ongoing experiment and plan to present the results of morphological changes and their effect on conductivity of films as the result of temperature changes on both samples. This work will also enable us to distinguish the substrate effects at higher temperatures.

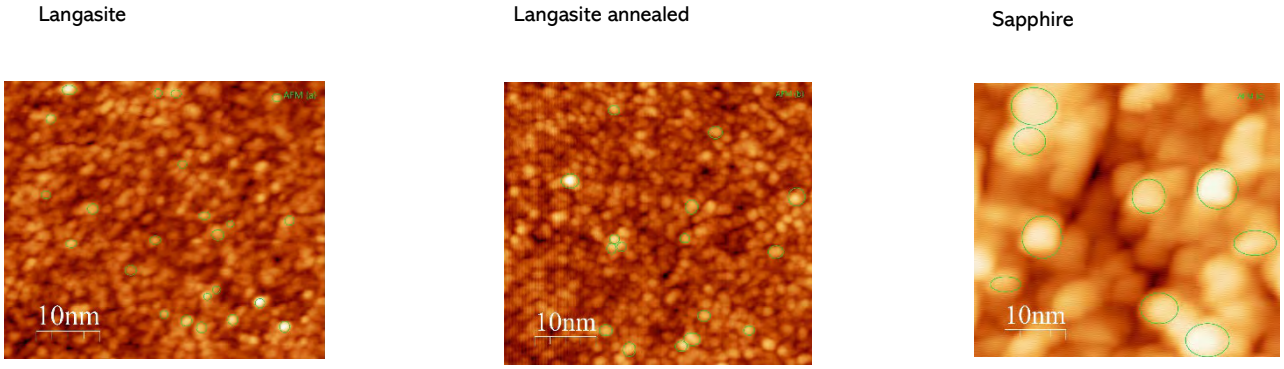

References:
[1] David J. Frankel, Scott C. Moulzolf, Mauricio Pereira da Cunha, Robert J. Lad, Surface and Coatings Technology, 0257-8972 (2015)
[2] Cunha, M. & Maskay, Anin & Lad, R.J. & Frankel, D.J. & Moulzolf, S. & Call, Michael & Bernhardt, G. IEEE International Ultrasonics Symposium (IUS)(2015)

Preference: Poster

Investigation of Thermal Resistivity of Chromium (III) Sulfide using Scanning Thermal Microscopy

Thomas Iken[1], Carlos Munoz[1], Mehmet Ozdogan[1], Nuri Oncel[1]

[1]Department of Physics and Astrophysics, University of North Dakota, Grand Forks, ND 58202

Email: Thomas.Iken@und.edu

Thermoelectric materials (TEMs) can directly convert waste heat into electricity. Therefore, they have attracted attention as an environmentally friendly solution to ever growing energy demand. Recently, there has been an interest to investigate the thermoelectric (TE) properties of magnetic transition chalcogenides, namely, improving their TE efficiency. Improving the conversion efficiency of TEMs depends on the dimensionless figure of merit $zT=\alpha^2 \sigma T/\kappa$, where α is the Seebeck coefficient and σ is the electrical conductivity and κ is the thermal conductivity of the material. One way of increase the zT value of a given material is lowering its thermal conductivity value. Using SThM (Scanning Thermal Microscopy), we measured the thermal resistivity of Chromium (III) Sulfide (Cr_2S_3) nanocrystals, a promising material for thermoelectric applications. Results of the study show an inverse relationship between thermal resistance and height, as well as a logarithmic increase in thermal resistance as a function of the nanocrystal radius [1].

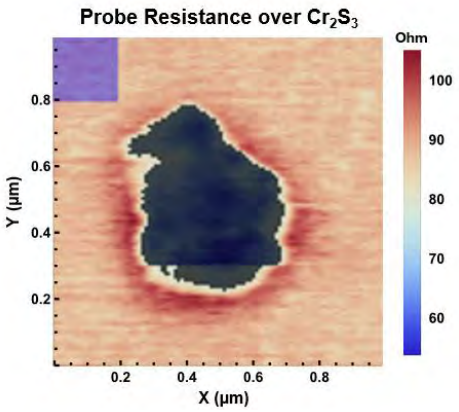

Fig. 1: Scan of Probe Resistance

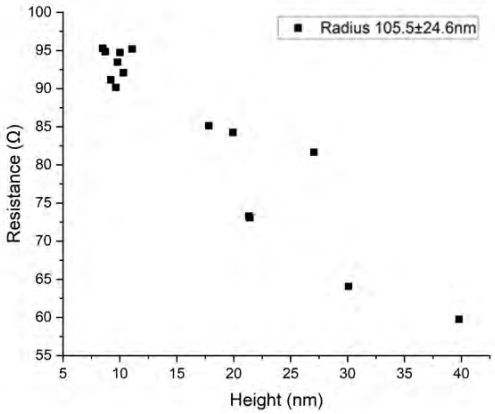

Fig. 2: Probe Resistance as a function of Cr_2S_3 height at

References:

[1] Jiang, M., Olarte-Plata, J. D., & Bresme, F. (2022). Heterogeneous thermal conductance of nanoparticle–fluid interfaces: An atomistic nodal approach. The Journal of Chemical Physics, 156(4), 044701. https://doi.org/10.1063/5.0074912

Preference: poster

Electrochemical Conversion of Carbon Dioxide to value-added chemicals on copper-based alloys

James Bartsch[1], Meredith Zannacker[1], Dong Hun Lee[2], Sunghwan Lee[2] and Sujat Sen[1]

[1]Department of Chemistry and Biochemistry, University of Wisconsin La Crosse, 54601
[2]School of Engineering Technology, Purdue University, West Lafayette, IN 47907

Email: jbartsch@uwlax.edu

Copper has been investigated extensively as an electrocatalyst for the conversion of Carbon dioxide (CO_2) to a variety of hydrocarbon products at room temperature. Alloys of copper (Cu) with metals such as silver (Ag) or tin (Sn) have also been shown to economically useful products such as ethylene, methane or formate with tunable selectivity between the same, depending on the composition of the alloy. Furthermore, varying the particle size, surface morphology, texture, and porosity of these catalysts have also been shown to dramatically change its electrocatalytic properties and product distribution.

In this work, we utilize thin layers of copper, silver and specific combinations of the same on both metal and gas-diffusion layer (GDL) substrates. Detailed characterization of these metal coated substrates has been done through scanning electron microscopy (SEM) as well as Energy-dispersive X-ray (EDX) analysis to determine relative ratios of the metals present. Herein, we present preliminary results showing the electrocatalytic performance of these metal films for the conversion of CO_2 inside both liquid-fed conventional H-Cell reactors using both cyclic voltammetry and chronoamperometry testing over 1-hour long electrolysis. Product analysis is performed through NMR for liquid phase products and GC-FID/TCD for gas-phase products. We also present on the characterization of these films after the electrolysis to understand changes to the metal surface and morphology.

Preference: poster

Substrate effect in on-surface reactions of conjugated organic molecules

Kai Wang, Soumyajit Rajak, Dairong Liu, Jeremy Schultz, Linfei Li, Nan Jiang

Department of Chemistry, University of Illinois Chicago, 845 W Taylor St., Chicago, Illinois, 60607, USA

Email: kwang81@uic.edu

Conjugated organic molecules are attractive candidates to realize platforms on surfaces, where self-assembly and molecule-substrate interactions can be used to impart tailored characteristics at the interface. Specifically, surface-catalyzed reactions that involve the dissociation of bonds within molecules can be used to demonstrate molecule-substrate interactions. Here, we use ultrahigh vacuum scanning tunneling microscopy (UHV-STM) to study the reactivity of three different organic molecules on transition metal surfaces. Firstly, N,N-diphenylquinodimethyl thioamide (Ph_2QDM) are found to desulfurize on Ag(100) rather than Au(111) or Au(100) surfaces, indicating the catalytic ability of the Ag surface in C=S cleavage. Furthermore, octaethylporphrin (OEP) molecules are employed to demonstrate dehydrocyclization processes on various metal surfaces with distinct energetic properties. Additionally, some reactions may show isomer selectivity. After annealing 3,6-dibromo-phenanthrenequinone (DBPQ) molecules on Au(100) surface, the coupling reaction has a selectivity toward *trans* dimers on bromine islands, while only *cis* dimers are observed on the undecorated Au surface. Consequently, our research shows that on-surface reactions are highly dependent on the surface structure, suggesting a potent way to controlling the reaction pathway or growth of nanostructures on surfaces.

Preference: Poster

Surface Structures of α-Quartz Prepared by Annealing and Chemical Etching

Y. Cho*, X. Li*, K. M. Burson

Physics Department, Grinnell College, 1116 8th Street, Grinnell, IA, 50112, USA
*co-presenters

Email: bursonkr@grinnell.edu

Crystalline silica (SiO_2) surfaces play an important role in nature and technology, and are often used as substrates in scientific studies. Despite its importance, the surface structure of quartz remains poorly understood, especially on the experimental side. Applications and scientific structure may benefit from tailored surface structures. Surface structures depend heavily on the preparation approach. Here we present a survey of common preparation approaches for α-quartz (0001) and characterize the resulting surface structures.

We prepared mirror polished α-quartz (0001) by high-temperature annealing, cleaning with common solvents, and chemical etching approaches. Surfaces are then characterized using atomic force microscopy (AFM). The high temperature annealing (1200 °C) leads to well-defined, flat, and clean terraces in ambient conditions (Figure 1). Using AFM, we observed a large-scale surface termination with a reconstruction periodicity of 5 nm, consistent with previous literature [1,2]. The resulting surface structures from the high temperature annealing preparation will be compared with preparations for a mid-range temperature anneal (500 °C), below the alpha to beta transition for quartz, and with results from chemical cleaning and chemical etching. Understanding which surface structures result from each preparation creates a path towards tailored surface preparations for particular applications.

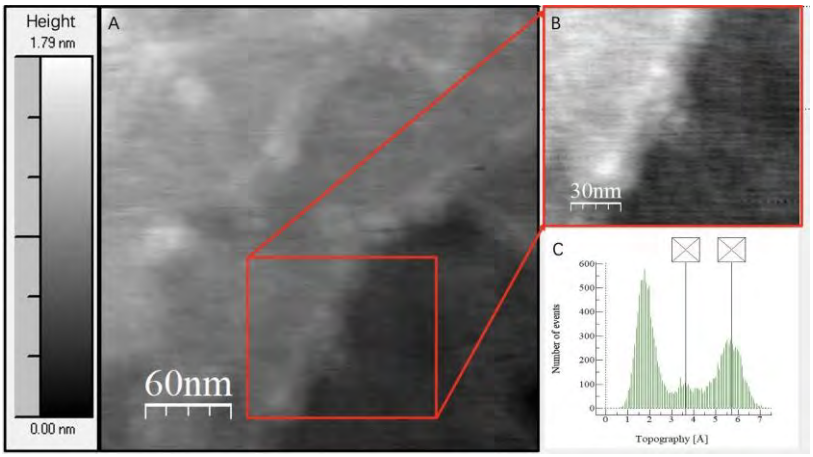

Figure 1: (a) Topography of alpha-quartz surface heated at 1100 °C for 24 hours. Flat terraces are visible. (b) AFM image of a single steps and (c) corresponding height histogram. Heights are consistent with the crystal structure along the c-axis.

References:
[1] Bart, F. & Gautier, M. *Surf. Sci.* 311, L671–L676 (1994).
[2] Eder, S. D. *et al. Sci. Rep.* 5, 14545 (2015).

Preference: poster

Conference: PEC 2023

Title: Adsorption and hydrogenation of 1,3-butadiene on Cu (111) and a Pd/Cu (111) single-atom-alloy

Mohammad Rahat Hossain
University of Illinois Chicago

Abstract:

A single atom alloy (SAA) is made by substituting catalytically active dopant metal atoms into the topmost atomic layer of a relatively inert host metal. Commonly, Pd and Pt are used for hydrogenation reactions due to their virtually zero barrier for H_2 activation. Yet, these catalysts are easily coked by CO and their high activity often limits their selectivity. Industrially, these catalysts are often doped with a less active metal to prevent coking and enhance their selectivity. One of the most important steps in the refinement of alkene streams for the industrial-scale production of high-quality polymers is the selective hydrogenation of 1,3-butadiene. In the literature, Pd (111) shows higher selective control over hydrogenation of 1,3-butadiene to butene than Pt (111). Therefore, the presence of isolated Pd atoms on a Cu host surface can be a suitable SAA catalyst model for this particular reaction. In this study, we used reflection absorption infrared spectroscopy (RAIRS) and temperature programmed desorption (TPD) to investigate the adsorption of butadiene and butene, as well as the hydrogenation of butadiene on Cu (111) and a Pd/Cu (111) SAA. The TPD study shows butadiene binds strongly to the Cu (111) surface compared to 1-butene. The desorption peak in the 120-130 K temperature range indicates the production of 1-butene from the hydrogenation of butadiene on the Pd/Cu (111) SAA. Auger electron spectroscopy (AES) shows no accumulation of surface carbon demonstrating molecular desorption of butadiene from the surface under UHV. The observation of both in-plane (CH_2-wag at 908 cm^{-1}) and out-of-plane (C-H bend at 1023 cm^{-1}) modes with RAIRS at monolayer coverage indicates that butadiene is adsorbed neither parallel nor perpendicular to the surface. In addition, IR peaks at 1464 cm^{-1} for ($-CH_3$) antisymmetric deformation and 1412 cm^{-1} for ($= CH_2$) scissors modes are observed on the Pd/Cu (111) SAA, indicating 1-butene formation from butadiene hydrogenation. The ambient pressure RAIRS studies are currently underway to calculate the turnover frequency (TOF) of the above-mentioned catalyst for the hydrogenation of 1,3-butadiene.

Can Whiskey Still Knowledge be Applied to Self-Assembled Monolayers?[1]

A. Molder[A], R. Bale[A], S. Pinnepalli[A], L. Espino[C], T. Portley[C], N. Oyler[A],M. Paquette[A], S. King[B]

[A]Missouri Institute for Defense and Energy, University of Missouri-Kansas City, Kansas City, MO
[B]Intel Semiconductor Corporation, Hillsboro, OR
[C]Sumner Academy High School, Kansas City, KS

Email: almvrd@umkc.edu

Self-assembled monolayers (SAMs) formed with unsaturated alkane thiols on gold have been well characterized and reported in the literature. SAMs have found themselves in retail consumer windshield washer fluid, oxidation protection and negative resists for lithography. Yet, the literature is devoid of investigations into SAMs with aromatic thiols on gold, and even thiols on Cu, a metal with arguably more relevant applications. By varying the tail group or incrementing the number of bridge carbons, we aim to optimize SAM order and maximize SAM coverage by vapor phase and solution chemistries and produce thermally stable, well-ordered surfaces with tunable surface characteristics.

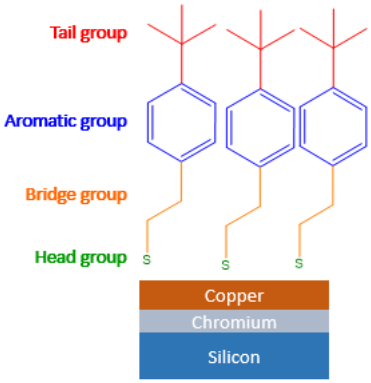

Our hypothesis is that one methylene carbon contained in the bridge group will produce the best packed/ordered/hydrophobic SAMs, as previously reported with aromatic thiols on gold.[2]

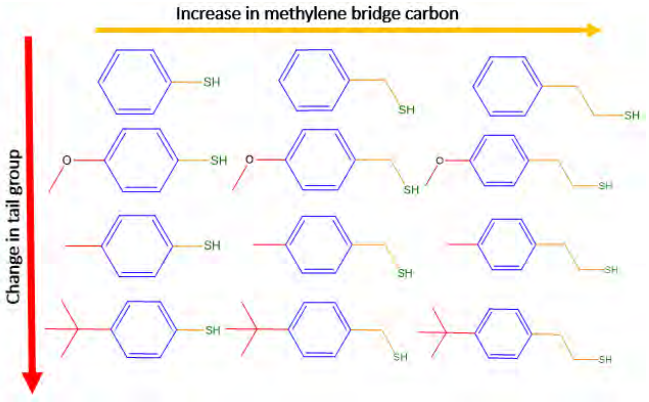

Our second hypothesis is that large hydrophilic tail groups will produce the most hydrophobic SAMs, although steric effects could show competing effects. We report here our investigation of this ancient love affair between copper and sulfur by XPS, water contact angle, AFM.

(1) Harrison, B.; Fagnen, O.; Jack, F.; Brosnan, J. The Impact of Copper in Different Parts of Malt Whisky Pot Stills on New Make Spirit Composition and Aroma. Journal of the Institute of Brewing 2011, 117 (1), 106–112. https://doi.org/10.1002/j.2050-0416.2011.tb00450.x.

(2) Tan, Y. S.; Srinivasan, M. P.; Pehkonen, S. O.; Chooi, S. Y. M. Effects of Ring Substituents on the Protective Properties of Self-Assembled Benzenethiols on Copper. *Corros Sci* **2006**, *48* (4), 840–862. https://doi.org/10.1016/j.corsci.2005.02.029.

Preference: Poster

Growth of Pd Nanoclusters on Single-Layer Graphene on Ir (111)

Buddhika S. A. Gedara, Shilpa Choyal, Nan Jiang, and Michael Trenary

Department of Chemistry, University of Illinois at Chicago, 845 West Taylor Street, Chicago, Illinois 60607

Email: awijen2@uic.edu

Metal nanoclusters formed on graphene or graphene-oxide templates have garnered significant attention in recent years. They have been extensively studied due to their wide range of applications in catalysis, biosensing, semiconductor devices, hydrogen storage, and electron transport. Nucleation and growth of Pd nanoclusters on a single-layer of graphene on the Ir(111) surface have been studied using scanning tunneling microscopy (STM). Dendritic Pd islands are grown on the Ir(111) surface, while triangular-shaped Pd clusters are grown on the graphene surface. Due to weak interaction between the underlying graphene and the Pd, Pd clusters are removed by the STM tip as shown in Fig. 1. This allows us to find the nucleation site of the Pd clusters on the supercell of the moiré superstructure. The lattice mismatch between the graphene layer and the underlying substrate surface gives rise to moiré structures, providing a variety of binding sites for adatoms and small clusters. We found that the Pd clusters nucleate at fcc sites (where the center of the graphene ring is located above the fcc hollow site of Ir(111)) on graphene.

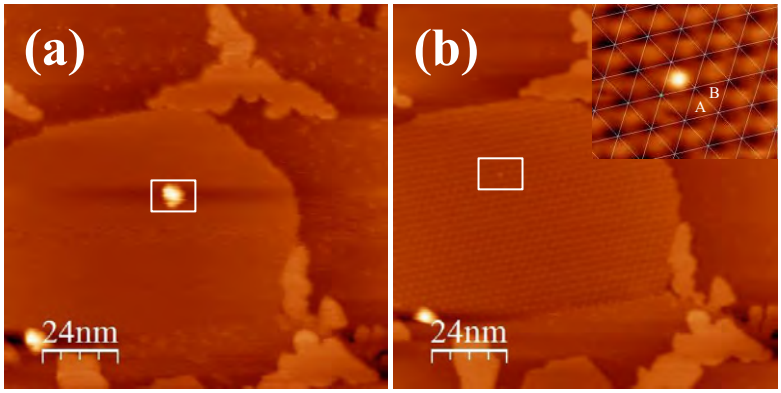

Figure 1. (a) A downward-pointing triangular Pd cluster on graphene is shown within the white rectangle box. (b) The Pd cluster has been removed from the graphene surface by the tip due to a weak interaction between the underlying graphene. The nucleation site of the Pd cluster is still visible as it presumably still contains few Pd atoms, and the inset demonstrates that this site is the fcc site (fcc and hcp regions are indicated by the A and B labels, respectively in the inset of (b)) on the supercell of the moiré superstructure. Images were recorded at 0.2 nA and 2.0 V in a 120×120 nm^2 area.

Preference: poster

Abstract for PEC 2023

In-Plane and Out-of-Plane Magnetic Behavior in Iron Borate Single Crystal

Jacob Pfund[1], Jacob Franklin[1], Joshua Bedard[1], Ilya Sochnikov[1,2] and Menka Jain[1,2]

[1]*Department of Physics, University of Connecticut*, *Storrs, CT 06269*

[2]*Institute of Materials Science, University of Connecticut*, *Storrs, CT 06269*

Iron Borate ($FeBO_3$) is a unique material with promising applications in magnetic memory and magneto-optical devices. Single crystal of FeBO3 is transparent and green with rhombohedral calcite-type structure (space group D_{3d}^6). It is a room temperature ferromagnet with an optical band gap of 2.9 eV and plate-like growth. Neutron studies have shown that $FeBO_3$ becomes antiferromagnetic (AFM) below T_N ~348 K, with weak ferromagnetism in which the magnetic moments of the sublattice lie in the basal plane. However, there is lack of in-plane and out-of-plane magnetic data at low temperatures. In this work, we present the detailed in-plane and out-of-plane magnetic behavior in single crystal of $FeBO_3$. Temperature-dependent magnetic measurements show applied magnetic field dependent behavior at low temperatures (T< 25 K). Low temperature SQUID images are presented to identify the canting of magnetic moments and novel behavior near the ground state. Detailed magnetic properties, such as magnetic moment, exchange interaction parameters, and canting angles are also calculated.

Fabrication and Characterization of Zinc-Phosphate-Hydrate Crystals Hydrothermally-Grown on Cu Metal Substrates

Y. Spiegelhoff,[1] F. Zemajtis,[2] E. Kheirandish,[1] K. Sobolev,[3] and N. Kouklin[1]

[1]Departments of Electrical Engineering, [2]Materials Science and Engineering, and [3]Civil Engineering, University of Wisconsin-Milwaukee, 3200 North Cramer St., Milwaukee, WI, 53211, USA

Email: lin43@uwm.edu

Although zinc phosphate have been well known for its excellent anticorrosive resistance, strong biocompatibility as well as chemical and mechanical stability, the optical and electrical characteristics of this compound received little attention. In addition, the used fabrication methods are lengthy, involve multiple precursors and require strict control over processing parameters such as temperature and pH. In this work, layered films of zinc phosphate hydrate were hydrothermally grown on top of Cu metal substrates at a low temperature and in an one-step application. The morphological, structural, and opto-electronic properties of the as-synthesized films were investigated thoroughly in the context of their opto-electronic device applications. In particular, X-ray Diffraction (XRD), Energy Dispersive X-ray (EDX), Scanning Electron Microscopy (SEM), and Transmission Electron Microscopy (TEM) were carried, and the results are to be presented and discussed. The light-emission characteristics were further examined by Photoluminescence Spectroscopy (PL) and Photoluminescence Excitation (PLE) measurements. The chemical composition of the as-grown films were identified to be a combination of $Zn_3(PO_4)_2 \cdot 4H_2O$ and $Zn_3(PO_4)_2 \cdot 2H_2O$. Even with the structural water, the films remain highly crystalline, and are also mechanically and chemically stable. The films demonstrate unexpectedly strong UV light emissions at ~377 and 383nm and also a broadband visible light emission centered at ~450nm. The dominant electronic excitation-emission transitions underlaying the PL peaks are believed to be the band transitions involving defect states. The films also exhibit an Ohmic I-V response, and an Arrhenius type transport with an activation energy of ~285meV was observed. The photoluminescence and charge transport results hold a promise for future use of the zinc phosphate hydrates in low-cost UV-visible light sensors and as UV light emitting material.

Band structure tuning of 2-d intercalated quantum materials and nanographenes

M. Kolmer[1], S. Chen[1], Y. Han[1], Y. Luan[1,2], J. Hall[1,2], Z. Fei[1,2], L.L. Wang[1], J. W. Evans[1,2], M.C.Tringides[1,2]

[1]Ames National Laboratory, [2] Department of Physics, Iowa State University, Ames IA 50011
Email: mkolmer@ameslab.gov

The goals of our activities are the tunable synthesis and characterization of nanoscale structures with predictive control of their morphology and geometry, to realize novel types of 2-d quantum materials. We focus on several graphene-based materials to establish the underlying principles for controlling their dimensions, structural uniformity, interface quality and interatomic interactions. Materials include: (i) on-demand metal-graphene heterostructures grown by targeted metal intercalation, with precise experimental tuning of metal location [1-5] (ii) Nanographene (NG) and graphene nanoribbons (NGR) generated by on-surface synthesis utilizing programmable chemical reactions of organic precursors, an ideal playground to test quantum materials physics in atomically precise systems. We realize targeted electronic band structures by developing synthesis protocols to control the bonding of the deposited atoms at pre-designed locations based on in-situ surface diffraction (LEED) and scanning tunneling microscopy (STM). Post growth characterization of the targeted band structures with spectroscopic techniques (scanning tunneling spectroscopy (STS), photoemission spectroscopy (ARPES), scanning near-field optical microscopy (SNOM)) is used to confirm targeted electronic effects. Density functional theory modelling is applied both to optimize synthesis, to attain predictiveness in the growth and to validate the expected band structure modifications.

Recent Publications

[1] Y. Luan, M. Kolmer, M.C. Tringides, Z. Fei, "Nanoscale infrared imaging and spectroscopy of hot-electron plasmons in graphene", *Phys. Rev. B* **107**, 085414 (2023).

[2] Y. Han, M. Kolmer, M.C. Tringides, JW Evans "Thermodynamics and kinetics of Pb intercalation under graphene on SiC (0001)" *Carbon* **5** 336 (2023).

[3] S. Chen, Y. Han, M. Kolmer, J. Hall, M. Hupalo, J.W. Evans, M.C. Tringides "Targeted Dy intercalation under graphene/SiC for tuning its electronic band structure" *Phys. Rev. B* **107**, 045408 (2023)

[4] M. Kolmer, B. Schrunk, M. Hupalo, J. Hall, S. Chen, J. Zhang, C.-Z. Wang, A. Kaminski, M.C. Tringides, "Highly Asymmetric Graphene Layer Doping and Band Structure Manipulation in Rare Earth–Graphene Heterostructure by Targeted Bonding of the Intercalated Gadolinium", *J. Phys. Chem. C*. **126**, 6863 (2022).

[5] M. Kolmer, W. Ko, J. Hall, S. Chen, J. Zhang, H. Zhao, L. Ke, C.Z. Wang, A.P. Li, M.C. Tringides "Breaking of Inversion Symmetry and Interlayer Electronic Coupling in Bilayer Graphene Heterostructure by Structural Implementation of High Electric Displacement Fields" *J. Phys. Chem. Lett*. **13**, 11571-11580 (2022).

[6] M. Kolmer *et al.* "Rational synthesis of atomically precise graphene nanoribbons directly on metal oxide surfaces" *Science* **369,** 571-575 (2020)

[7] M. Kolmer *et al.*, "Fluorine-programmed nanozipping to tailored nanographenes on rutile TiO_2 surfaces" *Science* **363**, 57-60 (2019)

Wednesday, August 2

9:00 AM – 10:40 AM

Hall of Nations Room 1300

Centennial Hall

308 16th Street North | La Crosse, WI 54601

Nottingham Prize Competition

Chair: Dr. Allee Marti, *WiSys*

Extended Abstract

Complexities at the spin state transition in molecular spin crossover complexes

Esha Mishra* **and Peter A. Dowben**

***Nottingham Contestant**

Department of Physics and Astronomy, University of Nebraska-Lincoln, 855 N 16th Street, Lincoln, NE, 68588, USA

Email: emishra@huskers.unl.edu

Molecular electronics is very compelling especially due to the fact that it may lend itself to green chemistry, provide efficient compact memory at low cost. Spin crossover molecules exhibits an unique feature of being able to switch between the distinct spin states, while changing conductance thus making spin crossover molecules a great candidate for nonvolatile memory devices. This conductance change provides a facile "readout" which, combined with robust voltage control at room temperature, makes molecular electronics based on spin crossover complexes potentially very valuable to the field of molecular electronics.

While working with the nonvolatile devices based on spin crossover complexes, it has been demonstrated, the microscopic mechanisms are not fully understood. Several spectroscopic techniques has been employed to investigate the possibility of an influence of magnetic field on the spin state change as well as to study the effects of different environments on the spin crossover molecules.

Transport properties of $[Fe(Htrz)_2(trz)](BF_4)$ plus polyaniline

Large resistance of most spin crossover molecules is a huge limitation when it comes to the performance of the molecular devices.[1] The addition of polyaniline has been shown to enhance the performance of the spin crossover complex $[Fe(Htrz)_2(trz)](BF_4)$ device by improving the conductance in the on-state, as seen in Figure 1 but it has been shown that this enhanced performance is the result of increased carrier mobility that leads to significaltly improved conductance.[2] The current voltage and capacitance voltage characteristics of the $[Fe(Htrz)_2(trz)](BF_4)$ plus polyaniline composite varies with spin state (Figure 1) with hole majority carriers.[2] While the addition of polyaniline preserves the $[Fe(Htrz)_2(trz)](BF_4)$ spin crossover

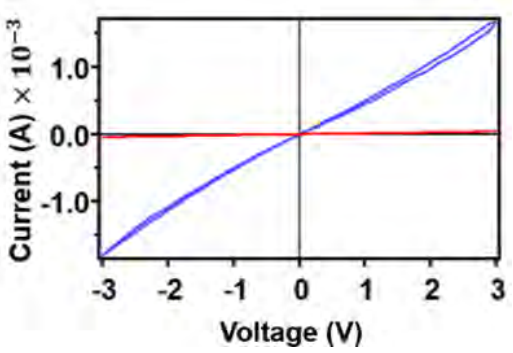

Figure 1: Current voltage characteristics of $[Fe(Htrz)_2(trz)](BF_4)$ plus polyaniline. 320 K and 380 K are represented by blue and red color respectively. From [2].

transistion the hysteresis and region of bistability decreases. Although the magnetic moment is local, in the high spin state, the change in spin state for some spin crossover complexes can influenced by not just voltage but magnetic field.

The effect of environments on the electronic properties of [Co(SQ)(Cat)(4-CN-py)$_2$] and [Co(SQ)(Cat)(3-tpp)$_2$

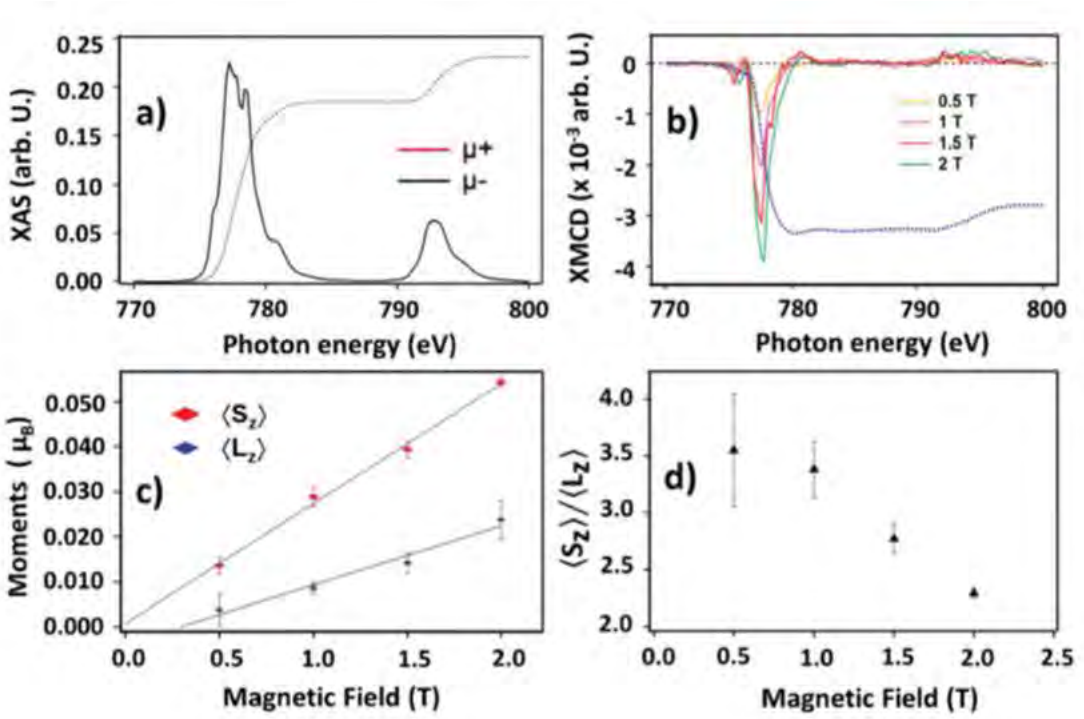

Figure 2: X-ray spectroscopy at 200 K of [Co(SQ)$_2$(4-CN-py)$_2$] on HOPG at Co L$_{2,3}$-edge. (a) X ray absorption spectra and (b) magnetic field dependent X-ray magnetic circular dichroism, (c) the spin moments and orbital moments with varying values of magnetic field. (d) the ratio of spin to orbital moment with varying magnetic field. From [3].

The magnetic field dependent X-ray magnetic circular dichroism (XMCD) of spin crossover [Co(SQ)$_2$(4-CN-py)$_2$] thin films indicates that at the zero magnetic field, there is absence of net spin moment, i.e. the system is paramagnetic. However, there ligand field effects and hints of preferential orinetation. Unlike the spin moment, the orbital moment of [Co(SQ)$_2$(4-CN-py)$_2$] in applied magnetic field indicates a significant nonzero value of the critical field,[3] as seen in Figure 2.

Optical excitations leading to a spin state change are also possible. In the case of the two cobalt based spin crossover molecules [Co(SQ)(Cat)(4- CN-py)$_2$] and [Co(SQ)(Cat)(3-tpp)$_2$], optically driven spin state changes are made possible by the existence of ligand to metal charge transfer state which can be identified through a comparison of ligand sensitive inverse photoemission and metal sensitive X-ray absorption.[4] The theoretical calculations derived from Density functional theory (DFT) has a good agreement with the experimental data obtained from several spectroscopic techniques. The change in the spin states of the spin crossover complexes led by the optical excitations is also validated by the orbital hybridization representing ligand to metal charge transfer states in Figure 3(b).

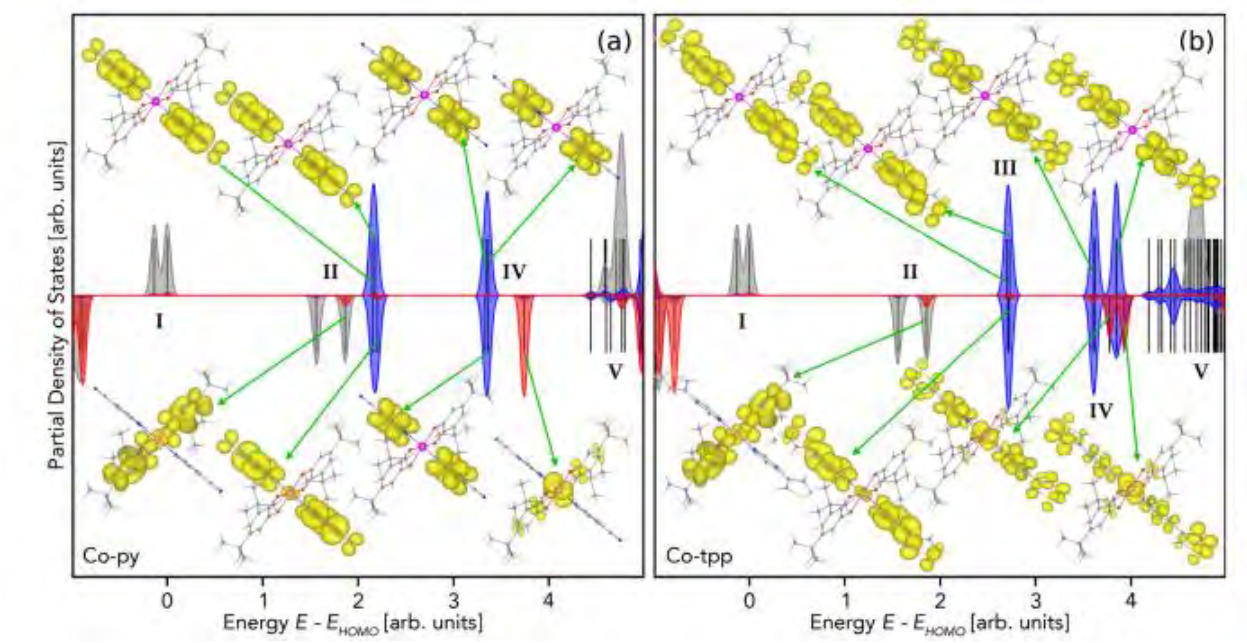

Figure 3: Partial density of states derived from ab initio Heyd–Scuseria–Ernzerhof calculations for high spin state (a) [Co(SQ)(Cat)(4-CN-py)$_2$]and (b) [Co(SQ)(Cat)(3-tpp)$_2$]. The contributions of cobalt, SQ ligand and 4-CN-py/3-tpp ligand are denoted in red, gray and blue colors respectively. From [4].

Additionally, the effect on the electronic structure of the two cobalt spin crossover tautomeric systems [Co(SQ)(Cat)(4-CN-py)$_2$] and [Co(SQ)(Cat)(3-tpp)$_2$], are little effected by the semiconducting polymer substrate (polyaniline (PANI) and a polar organic molecule, poly D lysine (PDL)) as characterized using the combination of spectroscopic techniques like optical absorption spectroscopy, X-ray Photoemission Spectroscopy (XPS), X-ray Absorption Spectroscopy (XAS) and Inverse Photoemission Spectroscopy (IPES).[4]

References:

[1] T. K. Ekanayaka, et al., *Magnetochemistry* **7** (2021) 37.
[2] E. Mishra, et al., *Organic Electronics*, **105** (2022) 106516.
[3] T. K. Ekanayaka et al., *Chem. Commun*. **58** (2022) 661.
[4] E. Mishra, et al., *Nanoscale*, **15** (2023) 2044.

Flexomagnetism and strain induced superconductivity in rippled GdAuGe Heusler membranes.

Z. LaDuca[1]* and J. K. Kawasaki[1]

***Nottingham Contestant**

[1]Department of Materials Science and Engineering, University of Wisconsin – Madison, 1550 Engineering Dr, Madison, WI 53706, USA

Email: zladuca@wisc.edu

Elastic strain is a powerful tool for tuning the ferroic properties of materials, as it allows for a modulation of material properties without the introduction of defects and disorder to a material system.[3–5] Here, we demonstrate novel flexomagnetic responses i.e., the coupling between strain gradient and magnetism, and strain-induced superconductivity, in GdAuGe Heusler membranes (Fig. 1).

Strain engineering of materials properties has largely been limited to small, uniform strains, as bulk crystals and epitaxial films generally undergo plastic deformation with < 2% strain[6,7], and epitaxial films are limited to discrete values of strain defined by the substrate they are grown on. Furthermore, studying the effects of strain gradients on materials ferroic properties has proven to be a great challenge, as it is nearly impossible to control strain gradients in bulk crystals and epitaxial films.

Our approach is to utilize ultrathin (≤20nm) membranes of Heusler compounds to study the effects of strain and strain gradients on materials properties. Membranes have been shown to withstand strain states inaccessible to bulk materials or epitaxial films, such as extreme strains upwards of 10%[8] that are free of constraints, granting the ability of continuous strain tuning in arbitrary directions. Moreover, the membrane geometry allows for the previously inaccessible gradient strain, via bending, twisting, and rippling.[4,9] Strain gradients break inversion symmetry, a key parameter for Dzyaloshinskii-Moriya Interaction (DMI) induced chiral spin textures such as skyrmions.[10]

In this study, we present the successful synthesis of high-quality flexomagnetic GdAuGe membranes through van der Waals epitaxy on graphene-terminated germanium substrates. We employ a 3-step growth approach to satisfy the needs for controlled surface morphology, film stoichiometry, and atomic ordering. Controlled GdAuGe growth begins with a 5nm codeposition of poorly ordered GdAuGe seed at temperatures ≤50°C (Fig. 2a,d), followed by a 480°C anneal to improve crystallinity (Fig. 2b,e), and subsequent growth to reach a total film thickness of 20nm (Fig. 2c,f). In situ reflection high energy electron diffraction (RHEED) is used to characterize surface morphology and order during growth. Sharpening of the GdAuGe reflections (Fig. 2a,b) represents a transition from rough, weekly crystalline surface to a smooth well-ordered surface. Additional reflections in the RHEED pattern, denoted by red arrows, originate from 30° rotated domains of GdAuGe that result from 30° rotated domains of graphene on the Ge(111) surface. XRD following film growth show a dramatic increase in the intensity of all GdAuGe Bragg peaks, indicating excellent atomic ordering. High resolution XRD scans of the GdAuGe(004) Bragg peak (Fig. 2h inset) reveal Keissig fringes, indicating a sharp graphene-film interface and smooth surface morphology. SEM of a GdAuGe film grown using a seeded

growth method (Fig. 2i) confirms a smooth surface morphology. We believe a seeded growth method can be translated to other materials grown on the graphene to control film stoichiometry and morphology.

Following film growth, GdAuGe membranes are mechanically exfoliated from the graphene surface, onto pre-strained polyurethane tape. The polyurethane tape was subsequently relaxed, generating a sinusoidal ripple structure in GdAuGe membranes, therefore introducing strains and strain gradients within the membranes. Optical and atomic force microscopy were used to measure the amplitude and period of ripples in encapsulated and exposed GdAuGe membranes, respectively. Maximum strain gradients located at the peaks and valleys of the sinusoidal ripples were calculated using equation derived from Ref 7. Magnetic ordering in unexfoliated GdAuGe films and rippled GdAuGe membranes, was characterized using SQUID magnetometry. Unstrained GdAuGe films exhibit antiferromagnetic ordering below ~14 K. However, the introduction of strain gradient in the rippled membranes induces a significant alteration in the magnetic ground state, provoking ferro/ferrimagnetic ordering at moderate strain gradients of 3-60%/μm Specifically, ferro/ferrimagnetic ordering occurs at T = 75-94K, in addition to the antiferromagnetic ordering observed at T = 7.5-8.8K (Fig. 1).

Intriguingly, an increased degree of rippling in GdAuGe membranes, resulting in high strain gradients exceeding 200%/μm, manifests the Meissner effect – a distinctive characteristic of superconductivity – at temperatures ranging from 3.3-4.1K. Figure 3 shows representative magnetic characterization of superconductivity via SQUID magnetometry. Figure 3a, DC magnetic susceptibility v. temperature, depicts a strong diamagnetic response at 4.1K when measured in the warming direction with a 5Oe applied field. The full range of temperature dependent magnetization can be seen in Fig. 1b. Maximum strains are calculated to be ±1.5% at the peaks and valleys of the sinusoidal ripples, corresponding to a strain gradient of 200%/μm across the ripple bend. The strength of this response as well as the critical temperature at which diamagnetism is no longer present (denoted by green arrows) are observed to be field dependent, with stronger applied fields resulting in weaker diamagnetism and lower transition temperatures. Figure 3b, magnetization v. applied field, shows a similar trend. Repulsion of the applied field increases with the strength of the applied field, then decays to a positive linear slope, suggesting the presence of type II superconductivity[11,12] and indicating antiferromagnetic ordering above critical fields and temperatures. The presence of antiferromagnetic ordering alongside superconductivity in the magnetic phase diagram of GdAuGe (Fig. 1a) shows a striking resemblance to that of unconventional superconductors.[13,14]

At present, the microscopic origin of flexomagnetism and its effects on the thermodynamics of spin reorientation and phase transitions in these membranes remain unclear. Advanced spectroscopic measurements and magneto-transport experiments, combined with theoretical modeling, are planned to further investigate these phenomena in these rippled membranes.

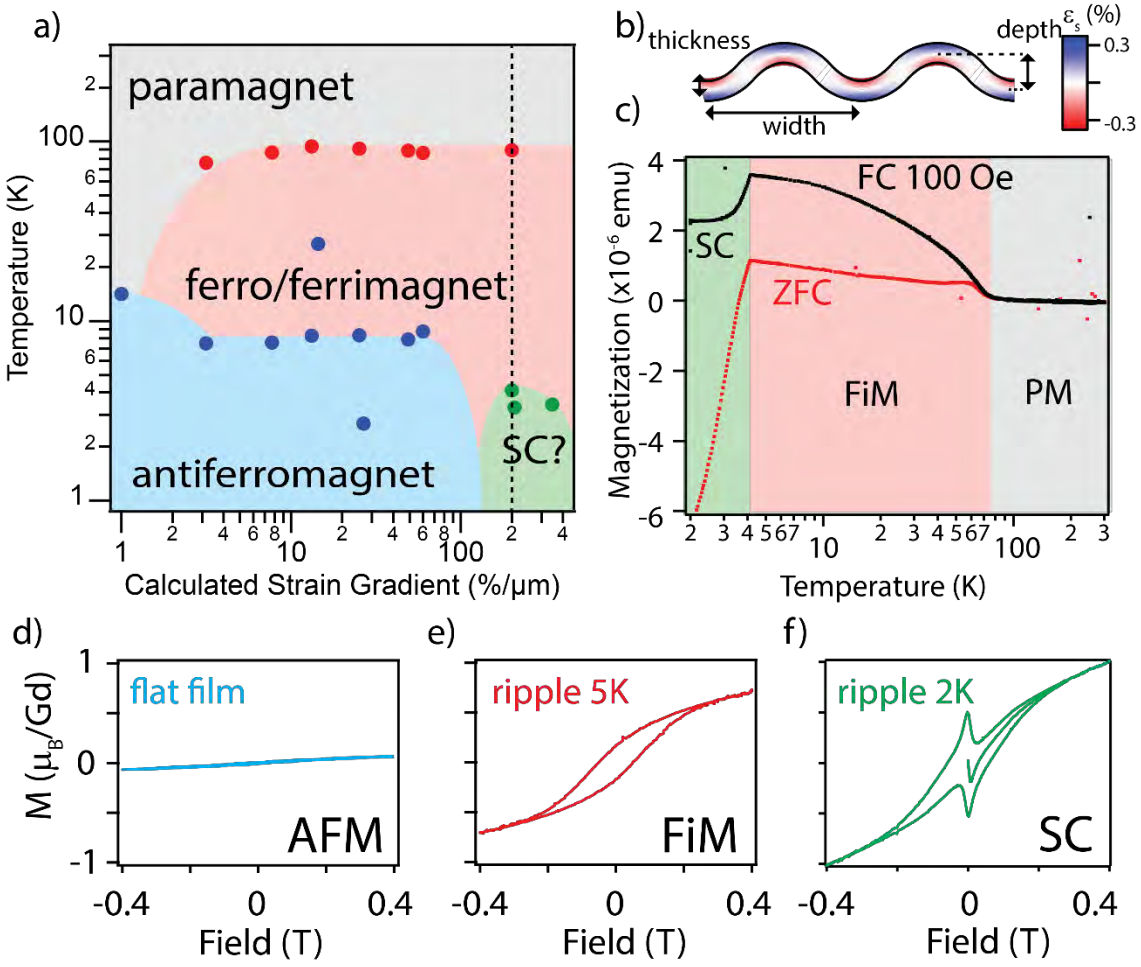

Fig. 1 Strain induced magnetism in GdAuGe. (a) Magnetic phase diagram of rippled GdAuGe membranes depicting antiferromagnetic ordering (blue), ferro/ferrimagnetic ordering (red), and superconducting critical (green) temperatures characterized by SQUID magnetometry. (b) Cartoon of rippled GdAuGe showing local tensile (blue) and compressive (red) strains. (c) Zero field cooling (red) and 100Oe field cooling (black) magnetization v. temperature scans of a rippled GdAuGe membrane, corresponding to the dashed line in (a). (d-f) Magnetization v. applied field for an unexfoliated GdAuGe film (d), rippled membrane above (e) and below (f) superconducting T_c.

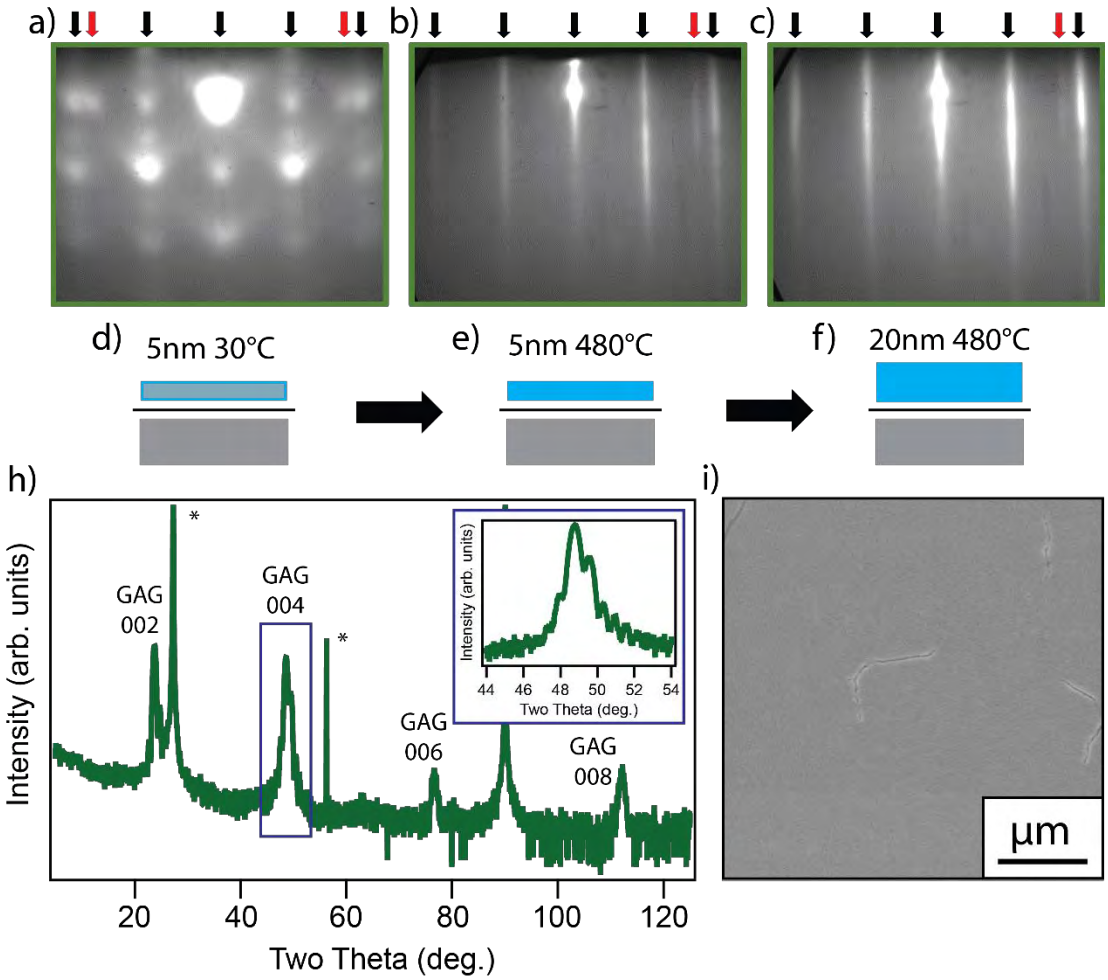

Fig. 2. Seeded epitaxial growth of GdAuGe. (a-c) in situ reflection high energy electron diffraction (RHEED) pattern along the GdAuGe<10$\bar{1}$0> azimuth after a 5nm seed layer deposition at 30°C (a), recrystallization by annealing at 480°C (b), and subsequent regrowth to a total of 20nm at 480°C (c). Black arrows mark reflections from the dominant in plane orientation of GdAuGe, while red arrows mark a secondary 30° rotated orientation of GdAuGe resulting from 30° rotated graphene on the Ge(111) surface. (d-f) cartoon representations of each step in our seeded growth approach. (h) Out of plane 2θ-ω XRD scans of a GdAuGe grown using our 3-step approach. Bragg peaks arising from the Ge(111) substrate are marked with asterisks. The inset shows a high-resolution scan of the GdAuGe(004) Bragg peak showing Kiessig fringes that result from sharp film interfaces. (i) SEM image of a GdAuGe grown using our 3-step approach, confirming a smooth surface morphology.

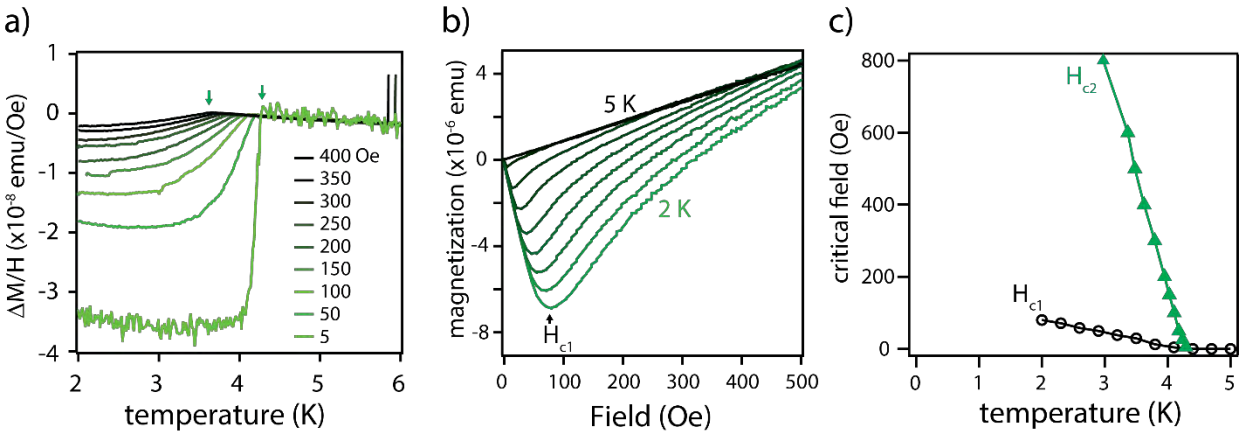

Fig. 3. Meissner effect in rippled GdAuGe. (a) DC susceptibility v. temperature measured by SQUID magnetometry in the warming direction showing field dependent diamagnetism in a highly strained, rippled GdAuGe membrane. Note the data has been rigidly shifted along the y-axis to better visualize the modulation of critical temperature with applied field. (b) Magnetization v. applied field measured at different temperatures by SQUID magnetometry. The apparent decay of diamagnetism with increasing field suggests the presence of type II superconductivity in GdAuGe membranes under extreme strain. (c) Temperature dependence of critical fields in rippled GdAuGe.

References:

1. Schlom, D. G. *et al.* Strain tuning of ferroelectric thin films. *Annual Review of Materials Research* vol. 37 589–626 Preprint at https://doi.org/10.1146/annurev.matsci.37.061206.113016 (2007).

2. Du, D., Hu, J. & Kawasaki, J. K. Perspective: strain and strain gradient engineering in membranes of quantum materials. (2023) doi:10.1063/5.0146553.

3. Kim, J. M. *et al.* Strain Engineering of Low-Dimensional Materials for Emerging Quantum Phenomena and Functionalities. *Advanced Materials* 2107362 (2022) doi:10.1002/ADMA.202107362.

4. Matthews, J. W. & Blakeslee, A. E. Defects in epitaxial multilayers: I. Misfit dislocations. *J Cryst Growth* **27**, 118–125 (1974).

5. People, R. & Bean, J. C. Calculation of critical layer thickness versus lattice mismatch for GexSi1−x/Si strained-layer heterostructures. *Appl Phys Lett* **47**, 322–324 (1985).

6. Dong, G. *et al.* Super-elastic ferroelectric single-crystal membrane with continuous electric dipole rotation. *Science (1979)* **366**, 475–479 (2019).

7. Du, D. *et al.* Epitaxy, exfoliation, and strain-induced magnetism in rippled Heusler membranes. *Nat Commun* **12**, (2021).

8. Zhang, Y. *et al.* Strain-Driven Dzyaloshinskii-Moriya Interaction for Room-Temperature Magnetic Skyrmions. *Phys Rev Lett* **127**, 117204 (2021).

9. Rjabinin, J. N. & Shubnikow, L. W. Magnetic Properties and Critical Currents of Supra-conducting Alloys. *Nature 1935 135:3415* **135**, 581–582 (1935).

10. Sarkar, M. R. H. & Naqib, S. H. Magnetic Field- and Frequency-Dependent Study of the AC Susceptibility of High-T c YBCO Single Crystal. *J Supercond Nov Magn* **35**, 1059–1070 (2022).

11. Norman, M. R. The Challenge of Unconventional Superconductivity. *Science (1979)* **332**, 196–200 (2011).

12. Cheng, J.-G. *et al.* Pressure Induced Superconductivity on the border of Magnetic Order in MnP. (2015) doi:10.1103/PhysRevLett.114.117001.

Probing Photophysical and Photochemical Processes via Nano-Confined Localized Surface Plasmons

Sayantan Mahapatra[1, 2] **and Nan Jiang**[1].

[1]Department of Chemistry, University of Illinois Chicago, 845 W. Taylor St., Chicago, Illinois 60607, United States.

[2]Current Address: Department of Chemistry, Northwestern University, 2145 Sheridan Rd, Evanston, IL, 60208, United States.

Email: sayantan.mahapatra@northwestern.edu

Probing physical and chemical processes at the sub-nanoscale level provides invaluable insights into chemistry-related fields such as molecular and catalytic systems, surface science, and biochemistry. As the basic building blocks of matter, the intricate details of atomic and molecular structure determine their behavior, in which, molecule–substrate and intermolecular interactions become extremely important. A slight change in the underlying surface could impact the molecular self-assembly drastically. As a result, comprehensive knowledge of structural and chemical properties is necessary to characterize the fundamental building blocks at the sub-nanoscale level.

As the surface analyzing technique, a scanning tunneling microscope (STM) provides the ability to image and manipulate individual molecules and atoms. By a complex analysis of the local density of states (LDOS), STM enables real-space topographic images of surface adsorbed systems. However, STM lacks chemical sensitivity. In addition, STM imaging typically provides meaningful topographic images if the molecules are aromatic and planar. For the non-planar flexible molecular skeletons, conclusive characterization of adsorption configuration may experience some issues. To address this, the STM measurements can be combined with near-field optical techniques. Specifically, the visible light can be focused on the plasmonic STM tip [1] to produce a highly localized and energetic electromagnetic (EM) field at the STM tip apex [localized surface plasmons (LSPs)], thereby enabling the chemical properties of the surface system with sub-nanoscale resolution in ultrahigh vacuum at low temperature (~78 K).

When illuminated with light, the intense LSP field confined at the STM tip apex enhances the traditionally weak Raman scattering process with an enhancement factor of 10^{12}-10^{13} for the surface system that resides underneath the tip. This yields angstrom-scale spatial resolution for tip-enhanced Raman spectroscopy (TERS) [2, 3, 4]. Again, the confined EM field can drive a thermodynamically unfavorable reaction under mild conditions, therefore significantly reducing the energy requirements for chemical transformation. In this work, confined LSP has been applied to the study and solution of various sub-nanoscale physical and chemical problems with a critical focus on the importance of angstrom-scale TERS and plasmon-mediated single-bond chemical reaction.

To begin, the real space angstrom scale chemical analysis of structurally regioisomeric porphodilactone molecules [*trans*- and *cis*-H_2F_{20}TPPDL, Figure 1] was performed on a Ag(100) surface, which lies at the heart of many heterogeneous catalysis reactions, modern-age electronic devices, and so forth [5]. The regioisomeric effect in porphodilactone (PDL), where two opposite pyrrole rings of porphyrin are oxidized to lactone moieties, plays an important role in modulating the photophysical properties of porphyrins. Firstly, the *trans*- and *cis*-isomers were separately investigated using STM on Ag(100). For *trans*-molecules, the STM image indicated a "pinwheel" conformation with a "regular" arrangement of the individual molecules (Figure 1a). Whereas the *cis*-isomers also took a "pinwheel" conformation while the packing in the self-assembly appears to be completely distinct ("zig-zag" pattern, Figure 1c). To set up the database first, a 633 nm incident laser irradiation was introduced to interrogate their vibrational properties separately as it is close to the actual excited electronic state of the molecule. Figures 1b and 1d show the Raman fingerprint, where significantly strong and intense peak features were discovered for the *cis*-isomers in the 500–900 cm^{-1} wavenumber region. Following that, we sequentially deposited both *trans*- and *cis*-H_2F_{20}TPPDL on Ag(100), and two distinct structures were found (Figure 1c, Structure 1 and 2). Because of the deposition of structurally similar skeletons, distinguishing them on the surface is now beyond the capacity of STM. However, with the high spatial resolution of TERS, it was possible to distinguish the vibrational fingerprints of molecules in each type of structural form. Through the implementation of Angstrom scale (8 Å) TERS line profile analysis, Structure 1 and 2 was found to manifest distinct change in the intensity of the 699 cm^{-1} peak, leading us to confirm roughly four molecules from Structure 1 (from points 1–7) are *trans*-isomers while about three molecules from Structure 2 (from points 8–11) island are *cis*-isomers (Figure 1f). Furthermore, a larger area was analyzed with TERS mapping, concluding the fact that these two regioisomers can self-recognize themselves, and they independently form separate ordered self-assembled structures within their van der Waals contact.

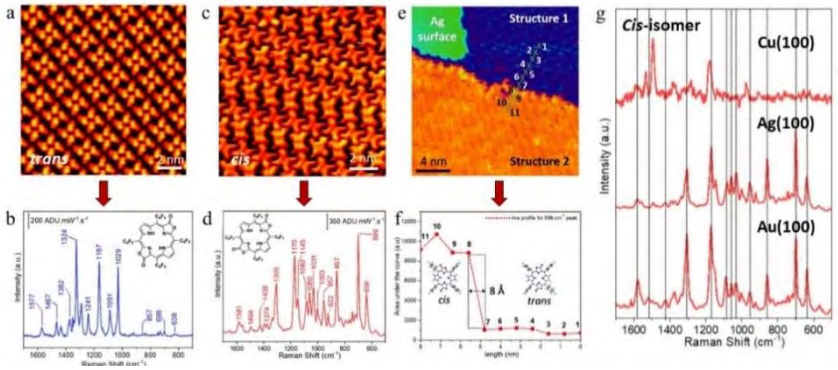

Figure 1. (a) and (b) STM image and TERS spectrum of *trans*-H_2F_{20}TPPDL. (c) and (d) STM image and TERS spectrum of *cis*-H_2F_{20}TPPDL. (e) STM image of co-deposited *trans*- and *cis*-isomers (Structure 1 and Structure 2). The points indicate the TERS line profile experiment. (f) Angstrom-scale (8 Å) TERS line profile. (g) comparison of TERS spectra of *cis*-isomer on Cu(100), Ag(100), and Au(100).

Although the conformation of PDL remains almost unchanged upon adsorption to the Ag(100), it becomes possible for the conformation of a molecule to change significantly when interacting with a surface. These molecules can exhibit nonplanar flexibility due to the rotation of σ-bonds or even C—C bonds that form their skeleton structure. The surface nanostructure formation significantly depends upon reliable control of these factors at the single-molecule level. To probe these molecule-substrate interactions at the sub-nanoscale level, Cu(100) and Au(100) substrates were

introduced [6]. Through STM-combined TERS experiments, a distinct adsorption configuration ("phenyl-flat") was identified on the Cu(100) substrate, as a result of significant molecule-substrate interactions. In comparison to the self-assembly formation on Ag(100) substrate via van der Waals interactions, the molecular self-assembly on Cu(100) was found to be stabilized via multiple C—F···F types of halogen bonding interactions. Again, on Au(100), the molecular orbitals of individual molecule could be imaged by STM because of the relatively weak molecule-substrate interactions. However, The TERS spectra acquired on Au(100) substrate showed excellent similarities (Figure 1g) with the spectra observed on Ag(100), leading us to conclude the adsorption configuration on Au(100) is similar to Ag(100).

Significantly strong interaction with the underlying surface can also chemically modify the molecule's framework, which introduces more complexity in the self-assembly formation. In an effort to enlighten this research area, ferrocene dicarboxylic acid (FcDCA), with applications for molecular spintronics, was investigated on Cu(100) [7]. FcDCA consists of two —COOH functional groups in the ferrocene backbone. STM imaging revealed the formation of a unique self-assembled structure. TERS measurements in combination with theoretical simulations revealed that the single FcDCA inside the self-organized assembly were chemically transformed during deposition due to strong molecule-substrate interactions. The rapid dehydrogenation process from the —COOH was found to occur on the Cu(100) substrate (Figure 2a). TERS provided vibrational fingerprint of the FcDCA where it was found to adsorb in a dipodal fashion with four Cu—O bonds.

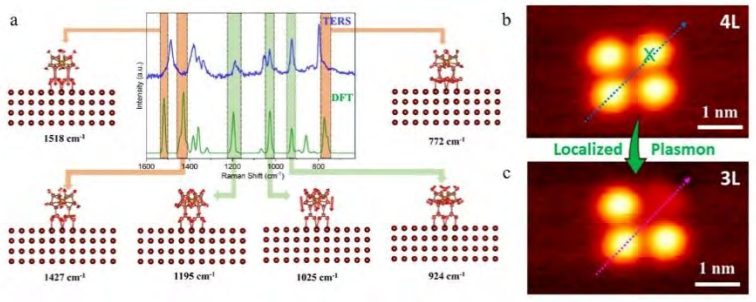

Figure 2. (a) Experimental TERS and DFT simulated spectra of FcDCA on Cu(100). Vibrational normal modes are identified. (b) and (c) STM image of 4L and 3L. The green cross in Figure 2b identifies the tip position for plasmonic treatment.

So far, utilizing visible light, examples on TERS have shown that the light scattering process can be enhanced by orders of magnitude for a molecule trapped between the plasmonic tip and a metallic surface. Along with amplifying the light-scattering process, chemical reactions induced by LSP are another promising application of plasmons, which has immense importance in promoting solar energy to chemical energy conversions. Here, a specific chemical bond (C—Si) bond inside a single molecule was activated by the LSP that was generated at the STM tip apex [8]. The nano-confined plasmons triggered one C—Si bond dissociation, in presence of multiple chemically equivalent active sites inside the single molecule. Following the plasmonic treatment by the STM tip, the four-lobe (4L, Figure 2b) structure of the intact TMSEP molecule was found to transform into a three-lobe (3L, Figure 2c) structure, resulting in the dissociation of one C—Si bond. Such plasmonic nano-confinement appears extremely crucial as the selective plasmon-induced chemical reaction was achieved at the sub-nanoscale level through our work.

Overall, the tandem technique of STM-TERS has advanced the sub-nanoscale analysis of surface nanostructures (via nano-confined LSPs) greatly in recent years, as explicitly described in the above examples. The inherently weak Raman signals can be amplified and utilized to solve various puzzles in the surface system which provides a consistent way to probe the sub-nanoscale physical and chemical properties. Additionally, the highly confined plasmonic field can be employed to activate chemical bonds with high precision and accuracy.

References:

[1] S. Mahapatra, L. Li, J. F. Schultz, N. Jiang, *J. Raman. Spectrosc.* **2021**, 52(2), 573-580. doi: 10.1002/jrs.5951

[2] S. Mahapatra, L. Li, J. F. Schultz, N. Jiang, *J. Chem. Phys.* **2020**, 153, 010902, 1-10. doi: 10.1063/5.0009766

[3] S. Mahapatra, D. Liu, C. Siribaddana, K. Wang, L. Li, N. Jiang, *Chem. Phys. Rev*. **2023**, 4, 021301, 1-16. doi: 10.1063/5.0143947

[4] J. F. Schultz, S. Mahapatra, L. Li, N. Jiang, *Appl. Spectrosc*. **2020**, 74(11), 1313-1340. doi: 10.1177/0003702820932229

[5] S. Mahapatra, Y. Ning, J. F. Schultz, L. Li, J-L. Zhang, N. Jiang, *Nano Lett.* 2019, 19, 3267-3272. doi: 10.1021/acs.nanolett.9b00826

[6] S. Mahapatra, J. F. Schultz, Y. Ning, J-L. Zhang, N. Jiang, *Nanoscale*. **2019**, 11, 19877-19833. doi: 10.1039/C9NR06830A

[7] S. Mahapatra, J. F. Schultz, L. Li, X. Zhang, N. Jiang, *J. Phys. Chem. C.* **2022**. doi: 10.1021/acs.jpcc.2c01434

[8] S. Mahapatra, J. F. Schultz, L. Li, X. Zhang, N. Jiang, *J. Am. Chem. Soc.* **2022**, 144, 5, 2051-2055. doi: 10.1021/jacs.1c11547

In situ surface characterization and modification of ZIF-8 films

Mueed Ahmad, [1,2,*] **and Jorge Anibal Boscoboinik**[1,2]

***Nottingham Contestant**

[1]Center for Functional Nanomaterials, Brookhaven National Laboratory, Upton, New York 11973, United States.
[2]Department of Materials Science and Chemical Engineering, Stony Brook University, Stony Brook, New York 11790, United States.

Email: mueed.ahmad@stonybrook.edu

Surface characterization plays a crucial role in understanding and optimizing the properties and performance of materials, including ZIF-8 (zeolitic imidazolate framework-8). ZIF-8 is a metal-organic framework (MOF) material that consists of metal ions (Zn^{2+}) coordinated tetrahedrally with organic ligands (2-methylimidazole, 2mIm hereafter) to form a porous crystalline structure. The surface properties of ZIF-8 can significantly influence its behavior and applications. Pore structure and surface area have been widely investigated by Brunauer-Emmett-Teller (BET) analysis as well as simulations in the past. Adsorption and diffusion studies on ZIF-8 films can be investigated by time-resolved Infrared reflection adsorption spectroscopy (IRRAS) coupled with mass spectrometry. Techniques such as X-ray photoelectron spectroscopy (XPS) enable the identification as well as quantification of different chemical species present on the ZIF-8 surface. The crystallinity of highly ordered ZIF-8 structures can be evaluated by the grazing incidence x-ray diffraction (GIXD) technique. At the same time, surface topography can be investigated by techniques like scanning electron microscopy (SEM) and atomic force microscopy (AFM) allows for the visualization of surface roughness, morphology, and particle distribution. The stability of ZIF-8 MOFs is of paramount importance for their successful operations in gas storage and separations[1], catalysis[2], and drug delivery applications. In contrast to stability, defects in ZIF-8 also alter their performance by enabling or removing adsorption sites for different gas molecules. The long-term permeance, structure integrity, and retention of porosity are vital for their practical applications in different fields, especially when it comes to replacing the conventional distillation method in gas separation applications.[3]

We are investigating ZIF-8 films/membranes using the above-mentioned techniques to further expand the understanding of the working of these novel materials in different environments. Our collaborators at Johns Hopkins University (JHU) have developed an all-vapor-based ZIF-8 synthesis method[4] that involves atomic layer deposition (ALD) of ZnO on Si-substrates and then converting ZnO-deposited samples into ZIF-8 by 2mIm vapor treatment at 120 °C in a custom reactor setup. We employed gold (Au) as a metal base layer to enhance the IRRAS signal due to the presence of a high dipole moment at the base. This enabled us to precisely investigate the fluctuations in the ZIF-8 chemical structure by tracking the changes in IR peak intensity and position from different functional groups in the material. The IRRAS spectra of ZIF-8 films with different thicknesses and a schematic of the ZIF-8 synthesis process are presented in Figure 1.

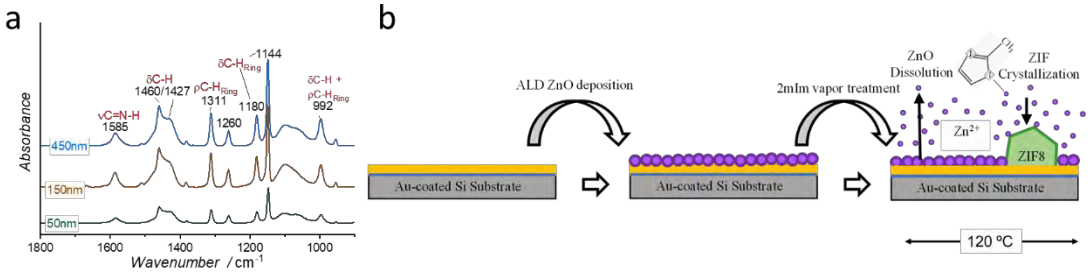

Fig. 1 – (a) The IRRAS spectra obtained from 50, 150, and 450 nm thick ZIF-8 film obtained in ultra-high vacuum (UHV) condition, (b) Schematic of ZIF-8 film synthesis process.

Our IRRAS instrument setup enables us to measure IR spectra under different environments to investigate the adsorption and desorption of different gases inside the ZIF-8 structure as well as to investigate the thermal stability of ZIF-8 films. We dosed propane, a renowned gas, for preliminary adsorption studies on ZIF-8 films. We cooled down the sample to 150 K using liquid N_2 and exposed our ZIF-8 films to 1E-5 mbar of propane. We measured IR spectra relative to propane exposure time on ZIF-8 and bare Au-Si substrate as a control sample. The difference IR spectra obtained by subtracting spectra at time zero are presented in Fig. 2a. The positive peaks can be clearly attributed to the adsorption of propane on Au as well as in ZIF-8 films. In contrast, the negative peaks present in ZIF-8 IR spectra can be resultant of the original peaks that are dampened due to the adsorption of propane on those sites. The intensity difference at the same exposure time between the Au-Si substrate and ZIF-8 sample is likely due to the high surface area of ZIF-8 films that can accommodate a greater number of propane molecules as compared to bare Au-Si substrate. Sequential scanning can be utilized to understand the kinetics of these gases' diffusion inside the ZIF-8 structure.

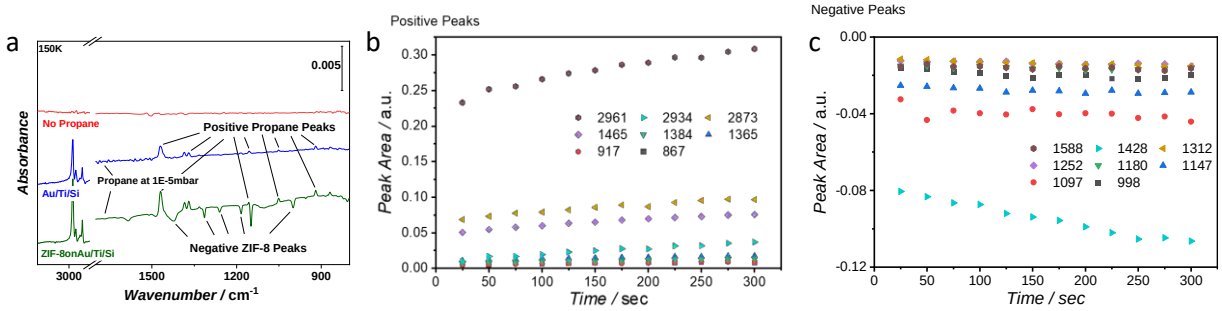

Fig. 2 – (a) Difference IR spectra obtained by subtracting IR spectra at exposure at time *t* with at time zero, (b) & (c) IR peak area change with respect to the propane exposure time.

We also investigated the modification of ZIF-8 films by thermal and non-thermal (plasma) techniques[5]. This allowed us to understand the limitations of the application of ZIF-8 films in different environments. The nonthermal plasma (NTP) process produces high reactivity at low temperatures and customizes the surface properties of materials. We used IRRAS with NTP to monitor in situ modifications in ZIF-8 thin films caused by oxygen and nitrogen plasmas. The IRRAS measurements in oxygen plasma uncover the progressive removal of the methyl group and imidazole ring from organic ligands, along with the formation of carbonyl moieties (C═O), as

shown in Fig. 1a. The peak around 1700 cm^{-1} kept on increasing with the plasma exposure time, suggesting the formation of carbonyl groups. Other observations were the appearance of the negative peaks from 1460 cm^{-1} (CH_3 bending), 1148 cm^{-1} (C-N stretching), and 1311 cm^{-1} (C-H bending from the ring), indicating the removal of ligands from the ZIF-8 structure. The presence of C═O moieties can make the ZIF-8 membrane more selective to CO_2 gas permeation due to enhanced Lewis acid−base and cooperative C−H−O hydrogen-bonding interactions between the anion in imidazolate and the carbonyl group. A nitrogen plasma, conversely, induces mild etching and grafting of nitrile groups (-C≡N), as shown in Fig. 1b. The optical images corresponding to O_2 and N_2 plasma are also presented next to IR results.

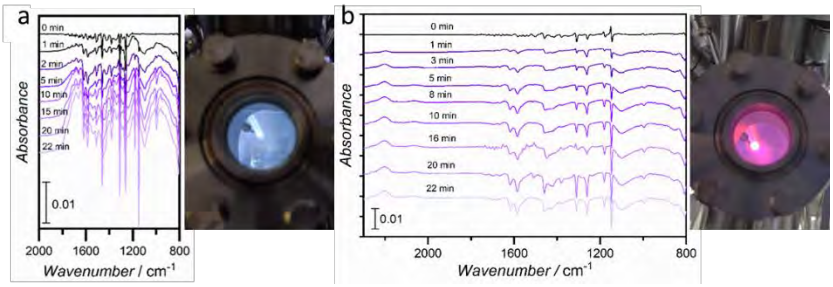

Fig. 1 – Difference IRRAS spectra (obtained by subtracting each spectrum at time *t* by the one at time zero) for (a) 10 W 0.1 mbar O_2 plasma and (b) 11 W 0.1 mbar N_2 plasma.

The effect of plasma power and exposure time in reference to peak areas for O_2 plasma can be seen in Fig. 2(a-c). The trend of reduction in peak areas with higher plasma power and exposure time validates the higher etching rates at these conditions. We also observed the formation of CO_2 in the gas-phase spectra that could largely be coming from the oxidation of organic legends and some oxidation of other carbonaceous species from chamber walls (Fig. 2d). Scanning electron microscopy (SEM) images of the ZIF-8 films treated under O_2 and N_2 plasma reveal the progressive etching occurring primarily at grain boundaries. Under similar conditions, N_2 plasma-treated ZIF-8 film's grain boundaries remain less affected, as shown in Fig. 2e and Fig. 2f.

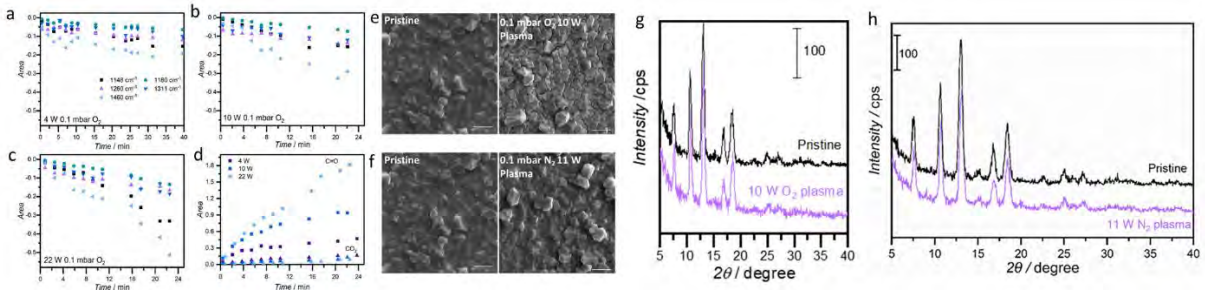

Fig. 2 – (a-c) Kinetics of ligand removal from ZIF-8 films under in situ plasma treatment at 0.1 mbar O_2 at 4, 10, and 22 W, respectively. (d) Formation of carbonyl and CO_2 groups under different plasma conditions. (e-f) SEM images of pristine and plasma treated ZIF-8 film under O_2 and N_2, respectively. (g-h) GIXD profiles after O_2 and N_2 plasma treatment, respectively.

Our collaborators at the University of Minnesota performed DFT analysis to assign IR assignments which we utilized as the basis for understanding the stability of ZIF-8 films. We also investigated

the changes in the IR peaks when defects are introduced into the ZIF-8 system to further expand our understanding of defects in the ZIF-8 structure. We compared simulated IR spectra from different ZIF-8 cases, including "defect-free", "Missing-Zinc," and "Missing-Linker" cases with experimentally obtained IR spectra from different ZIF-8 films/membranes and powder. Figure 3a(A-B) presents IR spectra obtained experimentally and through simulations. Figure 3b presents vibrational modes corresponding to IR peaks obtained from a "defect-free" ZIF-8 structure.

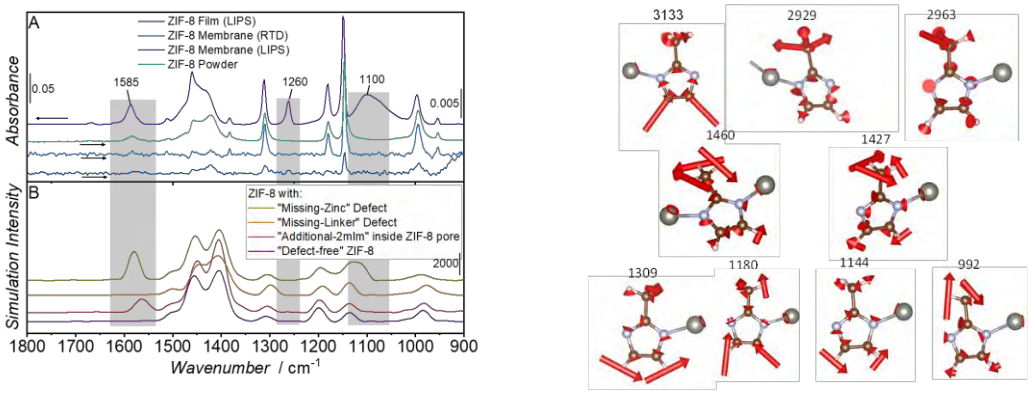

Fig. 3 – (a) IRRAS spectra obtained from ZIF-8 film/membrane/powder synthesized using ligand-induced Permselectivation (LIPS) as well rapid thermal dissolution (RTD) method, (b) Vector displacement diagrams obtained from defects-free ZIF-8 simulated structure. Vector here represents the displacement of atoms from their original position.

We also investigated the thermal stability of ZIF-8 films in oxidizing, inert, and in vacuum environments. We heated our ZIF-8 samples for 30 minutes at different temperatures while sequentially obtaining IR spectra. When heated in an oxidizing environment (0.1 mbar O2), we see positive peaks from difference IR spectra (shown in Fig. 4a) at lower temperatures up to 473 K. At 573 K, we start to see an abrupt reduction in the IR signal suggesting the degradation of ZIF-8 films. The regular IR spectra after each thermal treatment are presented in Fig. 4b. All peaks here show a redshift except for 1260 $cm^{-1,}$ which maintains its position. This shows that the 1260 cm^{-1} peak may not be related to the ZIF-8 structure. It is also to be noted that we do not see any peak at 1260 cm^{-1} from any simulated IR spectra.

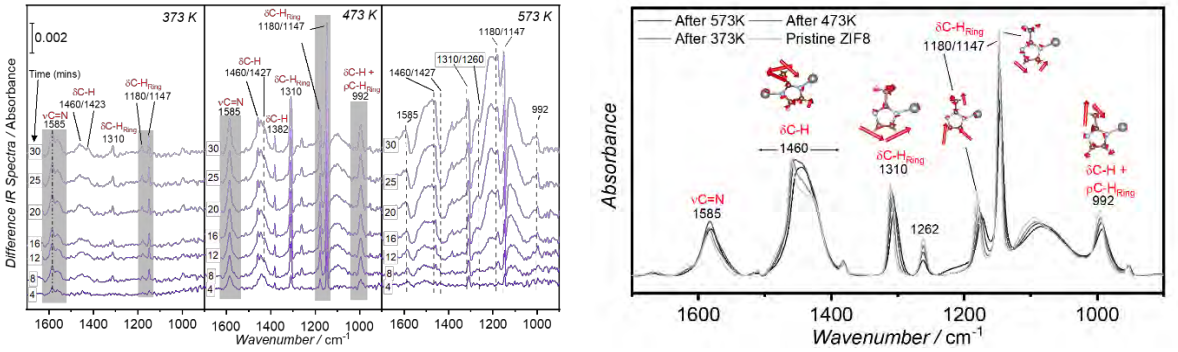

Fig. 4 – (a) Difference IR spectra during thermal treatment, (b) IR spectra at RT after thermal treatment.

We also exploited the XPS technique to further investigate the changes in stochiometric ratios during the modification of ZIF-8 films. Our setup opens the possibility of probing modifications in thin films at the surface as well as in the bulk region. We can now also investigate defects in MOFs which is crucial to fine-tune the performance of these materials. Further experiments are planned to expand our understanding of thin films and membranes for practical applications in the near future.

References

(1) Li, J.-R.; Sculley, J.; Zhou, H.-C. Metal–Organic Frameworks for Separations. *Chemical Reviews* **2012**, *112* (2), 869-932. DOI: 10.1021/cr200190s (acccessed 2023-05-02T15:06:42).
(2) Liu, J.; Chen, L.; Cui, H.; Zhang, J.; Zhang, L.; Su, C.-Y. Applications of metal–organic frameworks in heterogeneous supramolecular catalysis. *Chem. Soc. Rev.* **2014**, *43* (16), 6011-6061. DOI: 10.1039/c4cs00094c (acccessed 2023-05-02T14:23:14).
(3) Sholl, D. S.; Lively, R. P. Seven chemical separations to change the world. *Nature* **2016**, *532* (7600), 435-437. DOI: 10.1038/532435a (acccessed 2023-05-02T15:14:40).
(4) Miao, Y.; Lee, D. T.; Dorneles De Mello, M.; Abdel-Rahman, M. K.; Corkery, P.; Boscoboinik, J. A.; Fairbrother, D. H.; Tsapatsis, M. Electron beam induced modification of ZIF-8 membrane permeation properties. *Chemical Communications* **2021**, *57* (43), 5250-5253. DOI: 10.1039/d1cc00252j (acccessed 2023-06-21T21:00:51).
(5) Dorneles De Mello, M.; Ahmad, M.; Lee, D. T.; Dimitrakellis, P.; Miao, Y.; Zheng, W.; Nykypanchuk, D.; Vlachos, D. G.; Tsapatsis, M.; Boscoboinik, J. A. In Situ Tracking of Nonthermal Plasma Etching of ZIF-8 Films. *ACS Applied Materials & Interfaces* **2022**, *14* (16), 19023-19030. DOI: 10.1021/acsami.2c00259 (acccessed 2023-06-02T08:13:08).

Automating Scanning Probe Microscopy With Machine Learning Algorithms

S. Arias[1]*, S. Hollen[1†], P.Zahl[2]

***Nottingham Contestant**
†Advisor

[1]Department of Physics and Astronomy, University of New Hampshire, 9 Library Way, Durham, NH, 03824, USA

[2]Center for Functional Nanomaterials, Brookhaven National Laboratory, 735 Brookhaven Ave Upton, New York 11973, USA

Email: sarias@bnl.gov

Since the invention of the first scanning tunneling microscope at IBM Zurich, scanning probe microscopy (SPM) has revolutionized nanoscience. SPM techniques include a wide range of probes that can be used to measure the physical properties of a material like electronic, chemical, and magnetic signatures. The major drawback of these SPM techniques is that they are very time intensive. In order to collect any valuable data for scientific analysis, imaging parameters have to be optimized. Machine learning (ML) can train an artificial intelligence (AI) to perform tedious image optimization steps in SPM like finding features of interest and performing tip tuning procedures [1-3]. The AI can be taught to recognize patterns commonly seen in SPM images to perform experiments autonomously [4] and to help with data analysis [5,6]. These elements will help to build a fully automated SPM, but a framework is needed to integrate all these individual tasks into a single machine.

Here I present my work to create a modular framework that is to be the base for a fully automated SPM AI controller. Utilizing open-source machine learning platforms and computer vision tools I created machine learning models to perform SPM tasks. My work led to the creation of Auto-HR-AFM [7], an AI tool to automatically collect HR-AFM images of petroleum-based mixtures. I trained an instance segmentation model to teach Auto-HR-AFM how to recognize features in HR-AFM images. Auto-HR-AFM then uses that information to optimize the imaging by adjusting the probe-molecule distance for each molecule in the run. Auto-HR-AFM is the initial tool that will lead to fully automated scanning probe microscopy (SPM) experiments, from start to finish. This automation will allow SPM to become a mainstream characterization technique for complex mixtures, an otherwise unattainable target.

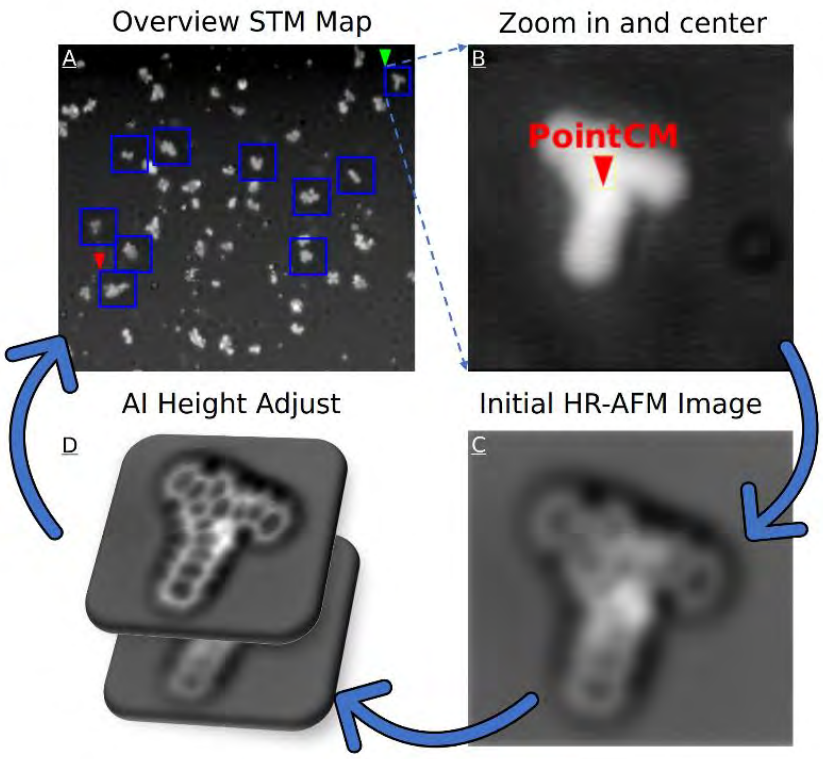

Figure 1: Auto-HR-AFM script architecture: A) STM map with queued to be imaged. B) Close-up STM image of the selected molecule using the center of mass to keep the molecule in frame. C) Auto-HR-AFM switches to HR-AFM to collect an initial image. D) Image from C) is passed through an ML algorithm to assess and then optimize the quality of the imaging. Once an optimal HR-AFM image is collected, Auto-HR-AFM continues with the next selected molecule.

Figure 1 shows the loop Auto-HR-AFM uses to collect an optimal NC-AFM image. Using an overview STM map of these petroleum molecules on Cu(111) shown in Fig. 1. A, a user selects single molecules for Auto-HR-AFM to collect optimized HR-AFM images of. Auto-HR-AFM takes a zoomed-in STM image (Fig 1. B) before taking an initial HR-AFM image (Fig. 1. C). In Fig 1. D Auto-HR-AFM assesses the initial NC-AFM image from Fig. 1. C through an ML algorithm and determines what action to take to collect a better image.

Auto-HR-AFM monitors the imaging conditions and reacts accordingly to get an optimized image similar to what an expert user would do. Auto-HR-AFM assesses the collected HR-AFM images using an instance segmentation model we trained using transfer learning starting from a Detectron2[12] archetype to recognize features on a single molecule.

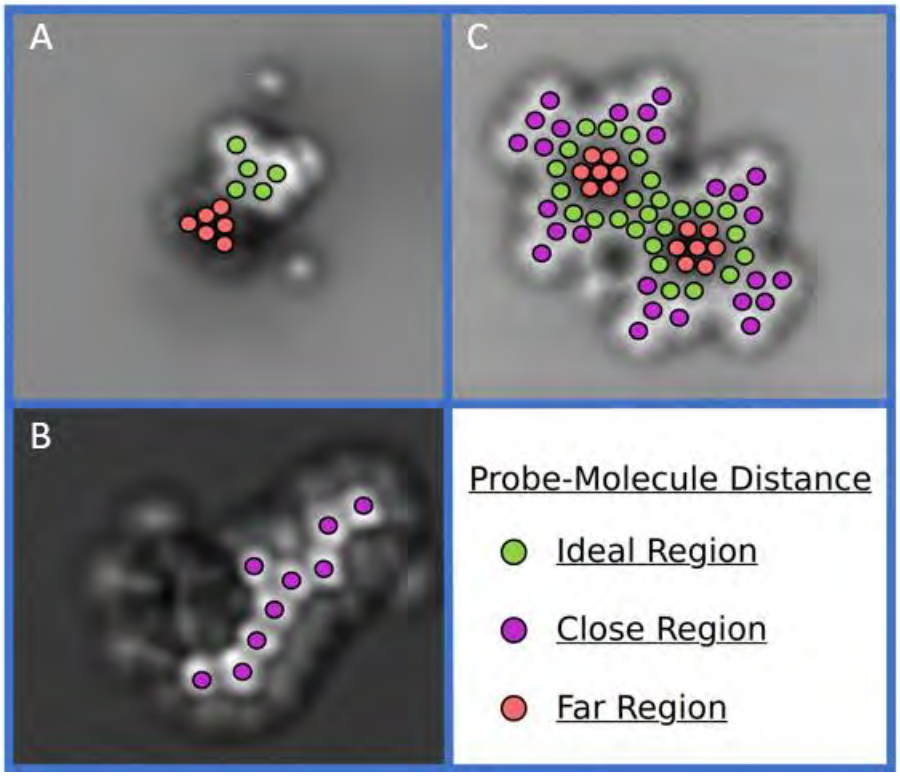

Figure 2: The three regions of probe-molecule distances Auto-HR-AFM is trained to detect. Regions with an ideal distance for optimal HR-AFM images are seen in green. Regions that are too close or too far away are seen in purple and red, respectively. (A,B) Hydrocarbons found in petroleum mixtures and (C) graphene nanoribbon.

My model segments the collected images into three different classes that characterize the proximity of the CO-functionalized probe to the molecule: too close (Purple in Fig. 2) , too far (Red in Fig. 2), or at an ideal distance for imaging molecules (Green in Fig. 2). The model outputs the number of pixels of the original image that corresponds to each class. Based on which class has the highest number of pixels Auto-HR-AFM uses, GXSM [13,14] open-source software is used to control the SPM, to move the probe to collect a more optimal image. Once the best image is collected, the SPM proceeds to collect images of the other molecules in the experiment until a complete data set is achieved. Our technique, which builds upon the SPM automation foundation that already exists [1-4], provides an open-source platform on which specific tasks can be combined to create a fully automated SPM capable of routine characterization of molecular mixtures.

Auto-HR-AFM's AI-guided, automated scanning for AFM imaging enables unsupervised imaging. Using Auto-HR-AFM will lead to more high-quality data being collected in the limited time frame SPM users are allocated per project. This is specifically useful at national labs where typical projects are only allocated one to two weeks at a time. This optimizes the use of the SPM and related resources needed to keep the system running. Most importantly, because imaging each molecule is automatically optimized, projects will achieve higher fidelity structure

interpretation, and also a more diverse data pool, since images of non-planar molecules are also collected.

Despite these advantages and significant improvements, future additions and improvements will be needed. First, adding more ML decision-making tools to Auto-HR-AFM will lead to a fully-automated SPM. Recent work automating SPM actions like navigation, tip-tuning, and spectroscopy [1-4] can be updated and integrated with Auto-HR-AFM to make the technique more broadly applicable.

Second, the use of HR-AFM to image and study individual molecules will help us understand the chemical structure of complicated molecules [15], identify the composition of complicated molecular mixtures [16], and differentiate heteroatoms [17]. Recent work using ML models to identify the chemical structure and determine the nomenclature of molecules imaged by HR-AFM [5,18] can be integrated into Auto-HR-AFM. By collecting multiple molecules at a series of different heights, we can use these as input for molecular identification techniques and identify molecules in real time.

Third, Auto-HR-AFM can learn to recognize more details in the HR-AFM images if we expand the three classes used in the instance segmentation model. By implementing more chemistry rules as we create more classes, the AI could recognize the number of carbon atoms in the rings of these molecules. Six-membered rings are most common and are expected for aromatic structures, five-membered rings are also possible, but three, four, seven, or eight membered-rings are rare and have not been reported. Also, all carbons need to satisfy tetravalency for most stable molecules, although other valencies are possible such as stable free radicals. Structures have to be consistent with their sources, formation conditions, or reactivities. For example, some aromatic structures are extremely reactive and unstable. Training a machine learning model to recognize these chemistry rules while scanning will facilitate the discovery of these unusual structures.

Our Auto-HR-AFM script is fully open-source and customizable, ready to be expanded for wide use. Potential next steps to improve Auto-HR-AFM would be to include other SPM ML tools like navigation and tip tuning [1-4] and to expand the different types of molecules that the script can recognize, specifically molecules without carbon rings, to perform other imaging projects. Combining these ML tools is the launching point for a fully automated SPM that can handle any molecular mixture characterization project from start to finish.

References:

[1] B. Alldritt *et al*, Computer Physics Communicatons 273 108258, (2022).
[2] S. Wang *et al,* Journal of Physical Chemistry, 125(6), 1384-1390, (2021).
[3] M. Rashidi *et al,* Mach. Learn.: Sci. Technol., 1, No. 025001 (2020).
[4] A. Krull *et al,* Communications Physics, 3(1), 1–8, (2020).
[5] J. Carracedo-Cosme *et al,* ACS Appl. Mater. Interfaces, 15, 22692−22704, (2023).
[6] B. Alldritt *et al,* Science Advances, 6, eaay6913, (2020).

[7] P. Zahl and S. Arias, Github repository:Pico-Pilot. https://github.com/pyzahl/pico-pilot, (2022).
[8] O. Gordon *et al,* Rev. Sci. Instrum., 90, 103704, (2019).
[9] O. Gordon *et al,* Mach. Learn.: Sci. Technol., 1, No. 015001, (2020).
[10] O. Gordon *et al,* Nano Lett., 20, 7688−7693, (2020).
[11] S. Farley *et al,* Mach. Learn.: Sci. Technol., 2, No. 015015, (2021).
[12] Y. Wu *et al,* Github repository: Detectron2. https://github.com/facebookresearch/*detectron2, (*2019).
[13] P. Zahl *et al,* Rev. Sci. Instrum., 74, 1222−1227, (2003).
[14] P. Zahl *et al,* J. Vac. Sci. Technol. B, 28, C4E39, (2010).
[15] N. Pavliček *et al,* Nat Nanotechnol*.,* 12 (4), 308-311, (2017).
[16] P. Zahl and Y. Zhang, Energy & Fuels, *33* (6), 4775-4780, (2019).
[17]Y. Zhang, Energy & Fuels, *35* (18), 14422-14444, (2021).
[18] N. Oinonen *et al,* MRS Bulletin **47**, 895–905 (2022).

Wednesday, August 2

11:00 AM – 12:00 PM

Hall of Nations Room 1300
Centennial Hall
308 16th Street North | La Crosse, WI 54601

Oral Presentations

Session 5

Chair: Prof. William Kaden, *University of Central Florida*

Probing Local Structural and Chemical Properties of Atomically Thin Two-Dimensional Materials via Tip-Enhanced Raman Spectroscopy

Nan Jiang

Department of Chemistry, University of Illinois Chicago, Chicago, IL 60607, USA

Email: njiang@uic.edu

*Invited Abstract

The chemical interrogation of individual atomic adsorbates on a surface significantly contributes to understanding the atomic-scale processes behind on-surface reactions. However, it remains highly challenging for current imaging or spectroscopic methods to achieve such a high chemical spatial resolution. Tip-enhanced Raman spectroscopy (TERS), which couples scanning tunneling microscopy (STM) and surface-enhanced Raman spectroscopy, provides such a powerful capability to concurrently harvest topographic and chemical information with single-bond sensitivity at the angstrom-scale. Herein, we use ultrahigh vacuum (UHV) TERS to measure the angstrom-scale interfacial interactions of a vertical Van der Waals heterostructure of borophene with tetraphenyldibenzoperiflanthene (DBP) molecules. TERS reveals subtle ripples and compressive strains of the borophene lattice underneath the molecular layer. The induced interfacial strain is demonstrated to extend in borophene by ∼1 nm beyond the molecular region by virtue of 5 Å chemical spatial resolution.[1] Furthermore, we use our method to probe the local chemical properties of oxidized borophene. The results show that single oxygen adatoms on borophene can be identified and mapped with ~4.8 Å spatial resolution and single bond (B–O) sensitivity.[2] In addition to offering atomic-level insights into the above-mentioned systems, our studies demonstrate UHV-TERS as a powerful tool to probe the local chemistry of surface adsorbates and interfacial structures in the atomic regime with widespread utilities in heterogeneous catalysis, on-surface molecular engineering, and low-dimensional materials.

Reference:

1. L. Li, J. F. Schultz, S. Mahapatra, X. Zhang. X. Liu, C. Shaw, M. Hersam, N. Jiang, "Probing interfacial interactions in an organic/borophene heterostructure with angstrom resolution", *Journal of the American Chemical Society*, 143, 38, 15624-15634 (2021).

2. L. Li, J. F. Schultz, S. Mahapatra, Z. Lu, X. Zhang, and N. Jiang, "Chemically identifying single adatoms with single-bond sensitivity during oxidation reactions of borophene", *Nature Communications*, 13, 1796 (1-9) (2022).

Molecular and Atomic Assembly at Surfaces: Design Strategies to Achieve Chemical Function

Yufei Bai,[1] David L. Wisman,[1,2] and Steven L. Tait[1]

[1] *Department of Chemistry, Indiana University, Bloomington, U. S. A.*
[2] *NAVSEA Crane, Crane IN, USA*
Email: tait@indiana.edu

The central theme of materials science is the dependence of function on structure, which our group explores in two-dimensional molecular systems at surfaces. The grand challenge is to leverage the composition and structure of a system to develop novel function. In molecular materials, the selection and positioning of specific functional groups will direct packing and stacking, which determine the electronic and chemical properties of molecular thin films and semiconductors. Design of molecular ligands for metal-organic complexation at surfaces can address the long-standing grand challenge of high selectivity in heterogeneous catalysis. Our group is working to develop principles of on-surface molecular self-assembly[1] and of metal-organic complexation[2] to gain new insight into molecular layers and new chemical activity at metal single-site catalysts.[3] This work involves close collaboration with multiple research groups to synergistically combine talent in design, synthesis, sample preparation, characterization, analysis, theory, and computational modeling. Our group uses a range of surface characterization tools to interrogate these systems under well-controlled environments, including scanning probe microscopy, photoelectron spectroscopy, vibrational spectroscopy, and mass spectrometry. We investigate systems under a variety of conditions: solution/solid interface, ultra-high vacuum, and flow reactor conditions at high temperature and high pressure.

Here, I will report on recent results in several aspects of this work. We have demonstrated the impact of conformational entropy in impeding self-assembly, but that this can be overcome with appropriate selection of co-solutes. Metal-organic complexes at surfaces can be designed to achieve single-site metal centers in which we can observe redox isomerism, control of metal oxidation state, transmetallation, and chemical spillover to the support. We have transferred this design concept for single-site catalysts to high-surface-area powder oxide supports and shown that these can operate as effective catalysts in solution and under gas flow conditions. Ongoing work will seek to extend understanding of these systems to achieve molecular thin films and single-site catalysts of greater complexity. For example, we are examining the use of 2D covalent organic frameworks as templates for surface catalysts.

We are actively looking for new collaborators, especially new postdocs and grad students.

References

[1] D. L. Wisman, H. Kim, C. Kim, T. W. Morris, D. Lee, and S. L. Tait, Chemistry – a European Journal **27**, 13887-13893 (2021). DOI: 10.1002/chem.202101611
[2] T. W. Morris, D. L. Wisman, N. Ud Din, D. Le, T. S. Rahman, S. L. Tait, Surface Science **712**, 121888 (2021). DOI: 10.1016/j.susc.2021.121888
[3] E. Wasim, N. Ud Din, D. Le, X. Zhou, M. S. Pape, G. E. Sterbinsky, T. S. Rahman, S. L. Tait, Journal of Catalysis **413**, 81-92 (2022). DOI: 10.1016/j.jcat.2022.06.010

Preference: Oral

Wednesday, August 2

1:20 PM – 3:00 PM

Hall of Nations Room 1300
Centennial Hall
308 16th Street North | La Crosse, WI 54601

Oral Presentations

Session 6

Chair: Prof. Nuri Oncel, *University of North Dakota*

Investigation of Adhesion Forces on the Surface of Borrelia burgdorferi Using AFM

M. Carlos[1], O. Mehmet[1], T. Yvonne[2], B. Catherine[2], O. Nuri[1]

[1]Department of Physics and Astrophysics, University of North Dakota, Grand Forks, ND 58202

[2]Department of Biomedical Sciences, University of North Dakota, Grand Forks, ND 58202

Email: carlos.munoz@und.edu

The Lyme disease spirochete, Borrelia burgdorferi (Bb), is the leading cause of arthropod-borne disease in the USA. Adhesion is important to the establishment of infection and contributes to dissemination, persistence, and immune evasion. Therefore, understanding bacterial adhesion at the molecular level is crucial. Atomic Force Microscopy (AFM) can provide both the topography and mechanical properties of biological samples. With AFM, we measured adhesive forces between non-functionalized AFM tips and adhesins on the surface of live Bb." Using contact-mode force spectroscopy we extracted the tip-bacteria adhesion characteristics of three different B. burgdorferi cell lines (Wild, A3D-DBL-KO, HPJ) with progressively higher mutations. From over 6000 total measurements, probability density functions for each mutant line were extracted and can be seen in Fig. 1 below [1]. Results of the experiment show significant adhesion forces between non-functionalized AFM cantilevers and B. burgdorferi, exhibiting a linear decrease in maximum adhesion with an increase in genes removed. Similarly, binding probability from successful vs unsuccessful adhesion events exhibits a linear decrease as a function of increased mutation.

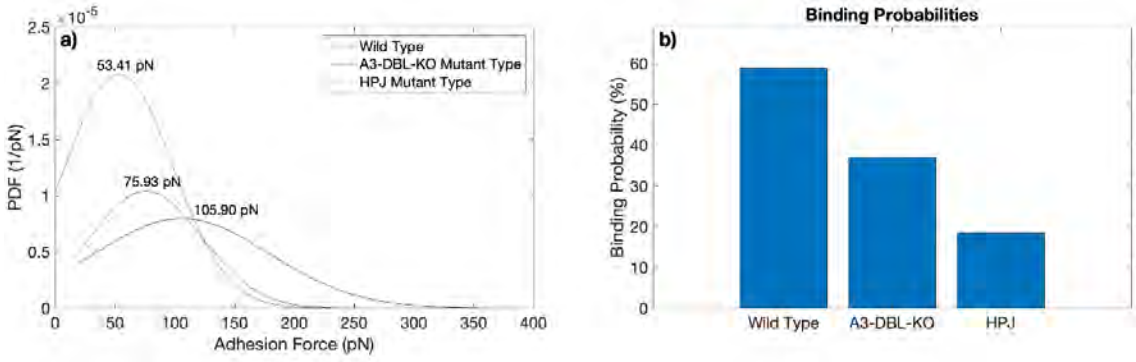

Fig. 1: Probability density function and binding probabilities

References:

[1] Viljoen, A., Mathelié-Guinlet, M., Ray, A., Strohmeyer, N., Oh, Y. J., Hinterdorfer, P., Müller, D. J., Alsteens, D., & Dufrêne, Y. F. (2021). Force spectroscopy of single cells using atomic force microscopy. *Nature Reviews Methods Primers*, *1*(1), 63.

Preference: oral

Catalyzed Degradation of Disinfection By-products on Iron Surfaces for Water Remediation

Kathryn A. Perrine* and Chathura de Alwis

Department of Chemistry, Michigan Technological University,

1400 Townsend Drive, Houghton, MI 49931-1295

*presenter

Email: kaperrin@mtu.edu

Abstract

Disinfectants are used to treat pathogens in water systems providing clean water to homes and communities. However chlorinated disinfectants react with humic acids and dissolved organic matter to produce halogenated hydrocarbons and halo-acetic acids, knowns as disinfection by-products products (DBPs). These toxic DBP's come in contact with iron interfaces that comprise soils through groundwater as well as cast iron pipeline infrastructures. Various ways for removal of DBP's include changing the disinfectant that is less oxidative or decomposition using catalysts. Zero valent iron is known to dehalogenate halohydrocarbons in the natural environment and is produced from reduction of iron materials or surface corrosion. During corrosion, iron undergoes a reduction-oxidation reaction leading to changes in chemical reactivity and surface topography, through pitting and deposition of corrosion products and inorganic film formation.

To understand the mechanistic pathways for mitigating chlorohydrocarbons, we investigated chloroform ($CDCl_3$), a model DBP, on Fe(111) at the gas/solid interface in ultra-high vacuum using a surface science approach. Using *in situ* infrared reflection absorption spectroscopy (IRRAS) and supporting density functional theory (DFT) predictions, we find that $CDCl_3$ physically adsorbs at -118 ˚C. Upon heating the $CDCl_3$ multilayer desorbs by -100 ˚C with an energy of 52.7 kJ/mol and the monolayer undergoes dissociative adsorption on Fe(111) above -53.8 ˚C with an energy of 67.5 kJ/mol. Additionally, Auger electron spectroscopy (AES) confirms the leftover Cl fragments from dissociation. The effect of water co-adsorption was measured and shows that adsorbed water blocks actives sites for $CDCl_3$ dissociation. The implications of this study are important for uncovering reactions on catalytic surfaces that address critical issues of water quality, remediation of contaminants, and its associated infrastructure.

Reference: de Alwis, C. and Perrine, K. A.; Surface Science 732 (2023) 122271

Preference: oral

Two-dimensional networks of halogen functionalized molecules on metal and semiconducting surfaces

M.C. Gallagher

Department of Physics, Lakehead University, 955 Oliver Road, Thunder Bay, ON, P7B-5E1, CANADA.

Email: mcgallag@lakeheadu.ca

Molecular self-assembly is one of the most important bottom-up fabrication strategies to produce two-dimensional networks at solid surfaces. The formation of complex two-dimensional (2-d) surface structures at the molecular scale relies on the self-assembly of functional organic molecules on solid substrates. Driven by an intricate equilibrium between molecule–molecule and molecule–substrate interactions, different non-covalent molecular interactions can be used to generate stable 2-d geometric structures.

In the case of halogen-terminated molecules, in addition to being the building blocks of self-assembled networks, the monomers can be activated to form 2-d π-conjugated polymers. Ideally this process follows a two-step procedure whereby the carbon halogen bonds break to form organometallic structures and subsequent covalent C-C coupling. These organic analogues of graphene, represent a promising new class of high-performance functional nanomaterials.

In this work we study the adsorption of tribromo-substituted heterotriangulene molecules on the (111) surfaces of Au, Ag and Si using room temperature scanning tunneling microscopy in ultrahigh vacuum. The resultant two-dimensional molecular networks range from: self-assembled networks held together by non-covalent interactions on the Au [1] and Si(111) $\sqrt{3} \times \sqrt{3}$-Ag surfaces; organometallic networks with C-Ag-C linkage on Ag; and a π-conjugated polymer when the monomers are deposited directly onto a hot Au(111) surface [2].

[1] G. Galeotti, *et al.* Synthesis of mesoscale ordered two-dimensional π-conjugated polymers with semiconducting properties. *Nature materials* **306**, 1–7 (2020).

[2] F. de Marchi. *et al.* Temperature-induced molecular reorganization on Au(111) driven by oligomeric defects. *Nanoscale* **295**, 2418 (2019).

Preference: Oral.

Fe and Cu deposition onto and intercalation into MoS_2

Jim Evans,[1,2] Dapeng Jing,[1] Michael Tringides[1,2] Marek Kolmer,[1] and Yong Han[1,2]

[1]Ames National Laboratory USDOE, Ames Iowa 50011

[2]Department of Physics & Astronomy, Iowa State University, Ames, Iowa 50011

Email: evans@ameslab.gov

Deposition of metals onto weakly-adhering layered materials is expected to result in the formation of 3D supported clusters (rather than 2D clusters) based upon predicted 3D equilibrium Winterbottom forms for such clusters. Indeed, 3D clusters are observed for Cu and Fe on MoS_2, although these exhibit non-equilibrium often geometric growth shapes [1]. These clusters include fcc(111) triangular pyramids for both Cu and Fe, and even clusters with a different bcc(110) crystal structure for Fe. The various cluster structures are characterized.

Deposition at high temperatures around 1000 K on MoS_2 surfaces subjected to Ar+ sputtering to create surface point defects can produce intercalated structures, at least for Cu [2]. For this system, we characterize the kinetic mechanism for intercalation ("seepage" through surface point defects to create a spreading intercalated carpet), and demonstrate the existence of (as well as quantifying) a low thermodynamic driving force for this process.

As an aside, we note that the mechanism and metal nanostructure morphologies are quite different for intercalation of these same metals for the layered material graphite (HOPG) [3].

References:

[1] D. Jing, A. Lii-Rosales, K.C. Lai, Q. Li, J. Kim, M.C. Tringides, J.W. Evans, and P.A. Thiel, Far-From-Equilibrium Growth of Metal Clusters on a Layered Material: Cu on MoS2, New J. Phys. 22, 053033 (2020).

[2] Y. Han, D. Jing, Y. Luan, C.-J. Wang, M. Kolmer, Z. Fei, M.C. Tringides, and J.W. Evans, Thermodynamically-driven Formation of Intercalated Cu Carpets from Supported Cu Pyramids on MoS2, J. Phys. Chem. Lett., 13, 6651-6656 (2022).

[3] A. Lii-Rosales, Y. Han, D. Jing, M.C. Tringides, S. Julien, K.-T. Wan, C.-Z. Wang, K.C. Lai, J.W. Evans, and P.A. Thiel, Encapsulation of Metal Nanoparticles at the Surface of a Prototypical Layered Material, Nanoscale, 13, 1485-1506 (2021).

The selective blocking of potentially catalytically-active sites on metal-supported iron oxide model catalysts

Dairong Liu[1], Linfei Li[1, 2], Nan Jiang[1]

[1]Department of Chemistry, University of Illinois Chicago, 845 W Taylor street, IL 60607, USA
[2]Department of Chemical Physics, Fritz Haber Institute of the Max Planck Society, Berlin 14195, Germany

Email: Dliu50@uic.edu

As one of the well-studied heterogeneous catalysts, iron oxides have found multiple applications in some of the most important catalytic transformations in the chemical industry. Among various types of iron oxides, ferrous oxide (FeO) has attracted immense interest due to its unique structural and chemical properties. Owing to its planar structure, the investigation of FeO benefits greatly from surface science techniques, such as scanning tunneling microscopy (STM). With the help of STM, the surface properties of ultrathin FeO islands grown on transition metals, particularly the role of the edges of these islands in catalysis (e.g., CO oxidation) have been well established. However, the metal affinity of FeO islands, which plays a crucial role in the fundamental properties of FeO-based metal/oxide catalysts, remains largely unexplored. Here, we study the interaction of Pd and Pt with FeO islands grown on Au(111) using STM. Different affinities of Pd and Pt with FeO are demonstrated by the preferential growth of Pd on the Fe-terminated edge and Pt on the O-terminated edge of FeO nanoislands, resulting in selectively blocked FeO edges. By revealing the distinct metal affinity of FeO edges, this work paves the way to the investigation of the catalytic properties of these unique metal-interfaced FeO edges, potentially shedding light on the design and modification of promising iron oxide catalysts.

Reference:

1) Ke Zhang[#], Linfei Li[#], Shamil Shaikhutdinov*, and Hans-Joachim Freund, *Angew. Chem. Int. Ed.* 57, 1261 (2018).
2) Ke Zhang[#], Linfei Li[#], Jacek Goniakowski*, Claudine Noguera, Hans-Joachim Freund, Shamil Shaikhutdinov*, *J. Catal.* 393, 100–106 (2021).
3) Dairong Liu, Linfei Li, Buddhika S. A. Gedara, Michael Trenary and Nan Jiang*, *Mater. Chem. Front.* 7, 476-482 (2023).

Preference: oral